12-2020

Rice Chilling Aeration: Assessment of Impacts on Grain Quality, Process Modeling and Validation

Soraya Shafiekhani
University of Arkansas, Fayetteville

Rice Chilling Aeration: Assessment of Impacts on Grain Quality, Process Modeling and Validation

A dissertation submitted in partial fulfillment
of the requirements for the degree of
Doctor of Philosophy in Food Science

by

Soraya Shafiekhani
Islamic Azad University, Tehran, Iran
Bachelor of Science in Food Science & Technology, 2010
Islamic Azad University, Isfahan, Iran
Master of Science in Food Science & Technology, 2014

December 2020
University of Arkansas

This dissertation is approved for recommendation to the Graduate Council.

Griffiths G. Atungulu, Ph.D.
Dissertation Director

Philip G. Crandall, Ph.D.
Committee Member

Sammy Sadaka, Ph.D.
Committee Member

Ruben O. Morawicki, Ph.D.
Committee Member

Christa Hestekin, Ph.D.
Committee Member

Rusty Bautista, Ph.D.
Committee Member

Abstract

The goal of this study is to demonstrate the effectiveness of applying chilling temperatures during on-farm, in-bin drying and storage to maintain rice quality. Specific objectives include to demonstrate the effectiveness of chilling aeration to preserve rice quality characteristics, determine the drying kinetics of rice under low temperature environments, and develop models to predict heat and mass transfer in rice kernel during drying at low temperature environment. To date, there is limited research describing storability or drying behavior of rice in chilled environments. However, it is understood that chilling of high-moisture, > 21% wet basis rough rice could reduce the time pressures on commercial and on-farm dryers to reduce the rough rice moisture content below 12% within two weeks of harvest. Chilling aeration of rice could also eliminate the pre-parboil steps where rice that has been dried to < 11% moisture, must be soaked in water to ~35-38% moisture prior to parboiling. Eliminating this initial drying step potentially reduces energy and operations costs. It is important to investigate suitability of chilling aeration for rice by considering implications on rice milling yields and quality, and process operation costs.

Acknowledgments

First and foremost, I have to thank my parents for their love, support, and prayers throughout my life. Thank you both for giving me strength to chase my dreams. My siblings, especially my brother Dr. Ali Shafiekhani deserve my wholehearted thanks as well.

I appreciate my advisor Dr. Griffiths G. Atungulu, for all his contributions and funding my course work and research. I also would like to appreciate all the support and the encouragement I received from my committee members including Dr. Sammy Sadaka, Dr. Rusty Bautista, Dr. Christa Hestekin, Dr. Philip G. Crandall and Dr. Ruben O. Morawicki.

I gratefully acknowledge the University of Arkansas' Division of Agriculture, the Grain Processing and Post-harvest Systems Engineering Program and the Rice Processing program for collaboration and providing facilities. I also acknowledge FrigorTec America Ins., especially through Mr. Jahannes Karcher for support and cooperation during the research. I also wish to acknowledge Mr. Mike Sullivan, Mr. Joe Mencer and Mr. Gregory H. O'Gary who provided rice samples and their facilities to conduct this research. This study was based on work that is supported, in part, by USDA National Institute of Food and Agriculture Hatch Act funding.

Thank you.

Soraya Shafiekhani

Dedication

To whom this may be an enlightenment.

Table of Contents

List of Tables

List of Figures

List of Published Papers

S. Shafiekhani, J. A. Lee, G. G. Atungulu. 2019. Predication of rice milling yield and quality attributes during storage using regression analyses. Transactions of the ASABE. 62(5): 1259-1268. (Chapter 2)

S. Shafiekhani, G. G. Atungulu. 2020. Effect of Rice Chilling on Drying, Milling and Quality Characteristics. Applied Engineering in Agriculture. 36(5): 767-776. (Chapter 3)

Chapter 1: **Introduction**

A considerable number of rice producers use on-farm, in-bin rice drying and storage facilities. The on-farm, in-bin rice management systems use natural air for conditioning or drying rice; if not managed properly, the rice processed using the system is prone to promote the development and contamination of the grain with mold which may lead to increased public health risk. To minimize the issues of rice deterioration, the trend among many rice growers in the U.S., in recent years, has been adoption of new processes in post-harvest production such as use of grain cooling/chilling systems. Chilling aeration presents an alternative method to chemical methods for preventing spoilage and insect infestation. While this technology has found use in other countries, application for use in the USA for rice has been hampered due to lack of scientific and industry relevant data. It is important to investigate suitability of this technology for rice by considering implications on rice milling yields, quality, and process operation costs. The objectives of this research were as following:

1. Development of models for more accurate prediction of kinetics of rice quality during on-farm, in-bin chilling aeration.
2. Determination of moisture removal, and changes in milling and quality characteristics of rice stored at chilled environment prior to treatment by conventional means.
3. Generation of new models for predicting equilibrium moisture content (EMC) isotherms of long-grain hybrid rice at chilled environment.
4. Conduct simulations to determine heat and mass transfer of long-grain hybrid rice under chilled environment.

Results for the first and second objectives are covered in the second and third chapters of this dissertation and have been published with titles “Prediction of rice milling yield and quality attributes during storage using regression analyses” and “Effect of rice chilling on drying, milling and quality characteristics”, respectively. Results from researches related to the third and fourth objectives are discussed in the fourth chapter of this dissertation with the title “Modeling heat and mass transfer of long-grain hybrid rice at chilled environment”; as of time of writing of this dissertation, this portion of the study has not yet been published.

Chapter 2: **Prediction of rice milling yield and quality attributes during storage using regression analyses**

Soraya Shafiekhani, Jung Ae Lee, Griffiths G. Atungulu

2.1 Abstract

Regression analyses were performed to determine the storage conditions that exhibited the best outcomes for long-grain, hybrid milled rice yield and quality. This study evaluated mold population on rough rice, milled rice discoloration, and head rice yield (HRY) after storage of rough rice in airtight conditions at moisture contents (MCs) of 12.5%, 16%, 19%, and 21% wet basis and temperatures of 10°C, 15°C, 20°C, 27°C, and 40°C at two-week intervals for 12 weeks. The experiment used a popular long-grain hybrid rice cultivar (XL745). Rice lots were procured from fields with and without conventional treatment of the field with fungicide for plant disease management. Field treatment and no field treatment were considered as a block, and a Mann-Whitney test was conducted to determine effect. The response surface method, an extension of second-order polynomial regression, was used to examine optimal treatment conditions. Mold population and milled rice discoloration from a combination of storage conditions were predicted using regression models. The first-order and second-order terms of temperature indicated a nonlinear relationship between temperature and ln(discoloration). The MC was positively associated with ln(discoloration), but the degree of impact may change with temperature because the interaction term was significant. From the model evaluation (R^2 and lack-of-fit test), the discoloration level is expected to be 57% (49% to 66% confidence interval) under conditions of 20% MC, 40°C, and nine weeks of storage for samples procured from fungicide-treated rice fields. This discoloration change is substantial compared to the initial discoloration of 9%. At high temperature (40°C) and MC (21%), discoloration started immediately after two weeks of storage.

Anaerobic storage conditions impeded mold growth, especially at high storage temperature (40°C). Low mold populations were observed in rice stored at low MC (16%). According to the regression model, the critical storage temperature that may lead to discoloration is between 27°C and 40°C. Pre-harvest fungicide treatment of rice in the field for disease control significantly improved the HRY but had no significant influence on mold population or discoloration. This study suggests a range of storage conditions to prevent losses in milling yield and quality of rice. In addition, the studied storage conditions mimicked the typical conditions for on-farm, in-bin drying and storage in the U.S. Mid-South, especially for the top layers of rice inside the bin, and therefore provide an important reference for growers and rice processors using in-bin structures to manage the quality of long-grain hybrid rice.

Keywords: Discoloration, Head rice yield, Mold population, Regression analysis, Rice quality, Rice storage.

2.2 Introduction

The USDA has established rice grades as U.S. No. 1 through U.S. No. 6. The grade is based on quality reduction factors (USDA, 2009). Damage and discoloration are listed in the USDA's quality evaluation criteria. Damaged rice is caused by insects as well as post-harvest processing (Vincent et al., 2008). Pre-harvest factors such as irrigation, nighttime air temperatures, rice cultivar, geographic conditions, and management as well as post-harvest factors such as moisture content (MC), temperature, and dockage can affect the quality of rice (Bason et al., 1990; Trigo-Stockli and Pedersen, 1994; Siebenmorgen et al., 2013; Atungulu et al., 2016; Shafiekhani et al., 2018).

Pinciroli et al. (2013) indicated that fungi growing on rice can cause discoloration. These fungi can be categorized as field fungi that infect rice before harvest and storage fungi that develop on

the grain after harvest (Neninger et al., 2003). Pinciroli et al. (2013) reported that field fungi were located in the hulls and bran layers, while storage fungi were mainly in the germ and endosperm. The development of storage fungi in stored grain is influenced by conditions of high moisture and high temperature and the amount of insect infestation. Mason et al. (1997) stated that rice starts to deteriorate from the time of harvest due to interactions among the physical, chemical, and biological variables in the environment.

One of the most important parameters for the rice processing industry is head rice yield (HRY). A head rice kernel is defined as a milled rice kernel with 75% (or more) of the length of a whole kernel (Marchezan, 1991; Ghadge and Prasad, 2012). Broken rice costs 30% to 40% less than whole kernels (USDA, 2018). To reduce the occurrence of fissures and improve the milling quality, proper post-harvest management of rice is critical (Sajawan et al., 1990; Dong et al., 2003; Debabandya and Satish, 2004; Rehal et al., 2017). Siebenmorgen et al. (1992) reported a correlation between HRY and rice kernel MC distribution at harvest. As harvest time progresses from early harvest dates to later dates, the MC of rice in the field generally decreases. The optimal HRY of long-grain rice is obtained when the rice is harvested at MC between 19% and 21% wet basis (w.b.).

Meullenet et al. (2000) presented regression models to demonstrate the effect of post-harvest variables such as MC, temperature, storage duration, and their interactions on rice sensory quality. Cooper et al. (2006) used regression models to describe the variation in rice milling quality with nighttime air temperatures. High daytime temperatures during the beginning of grain filling were detrimental to HRY, while high daytime temperatures at the end of grain filling increased HRY. Therefore, southern U.S. producers consider planting their rice crops earlier in the season, or

planting an early-maturing cultivar in July, which may prevent the HRY reductions associated with high nighttime temperatures during grain filling.

Kim et al. (2017) developed a prediction model for rice eating quality using physicochemical properties and sensory quality evaluation. They evaluated the eating quality of rice based on a rice palatability evaluation (RPE). The quality characteristic of milled rice (MR) and cooked rice (CR) were determined by moisture content, color, and hardness. According to the prediction model, the quality factors from the combination of MR and CR, rather than from either MR or CR alone, should be used to predict the eating quality of MR.

This study evaluated the individual and interaction effects of rough rice storage MC, temperature, and duration on HRY, discoloration, and mold population for samples procured from fields with different disease management practices to control microbes on the grain using pre-harvest fungicide treatments. The studied postharvest storage conditions mimicked the typical conditions for on-farm, in-bin drying in the U.S. Mid-South, especially for the top layers of rice inside the storage bin. Although numerous studies have reported optimal storage conditions for rice and the causes of rice quality loss, little research has been done to correlate HRY, discoloration, and mold population with rice MC, temperature, and storage duration for long-grain hybrid rice cultivars. Therefore, the objectives of this study were to (1) use a regression model to accurately predict the optimal conditions for rice storage and (2) investigate the impacts of pre-harvest, in-field treatment of rice with fungicide on HRY, discoloration, and mold population during rice storage.

2.3 Materials and Methods

2.3.1 Sample Preparation

Freshly harvested rough rice (long-grain hybrid XL745) from commercial field plots with and without pre-harvest fungicide application (Quilt-Xcel at the rate of 17 oz. per acre) was harvested

at 23% MC w.b. Rice samples from each plot were cleaned with a dockage tester (model XT4, Carter-Day, Minneapolis, Minn.). The cleaned rice samples were conditioned to MCs of 12.5%, 16%, 19%, and 21%. A conditioned environment chamber (26°C, 56% relative humidity) was used by placing the rice samples on a tarp in a stand-alone air conditioner (5580A, Parameter Generation and Control, Black Mountain, N.C.) to gently dry the samples to the desired MC. The MC of the samples was measured following the procedure in ASABE Standard S352.2 (ASABE, 2017), which involves drying 15 g of rough rice in an oven at 130°C for 24 h. After drying the rice samples to the desired MC levels, subsamples of approximately 300 g were placed in individually labeled sealed glass containers and transferred to five separate temperature environments (10°C, 15°C, 20°C, 27°C, and 40°C). The temperature environments involved an incubator (Binder Inc., Bohemia, N.Y.) for samples stored at 40°C, a conditioning chamber for the 27°C samples, and three refrigerators for the 10°C, 15°C, and 20°C samples. The samples were stored for 12 weeks, with samples taken every two weeks. Two replications were used for each storage condition.

2.3.2 Analysis of Milled Rice Yield and Quality

After removing the samples from storage, approximately 30 g subsamples from each sealed glass container were taken for fungi population analysis, and the rest of the samples were gently dried in a conditioning chamber (AA5582, Parameter Generation and Control, Inc., Black Mountain, N.C.) to 12.5% MC. This was done to standardize the samples for the subsequent quality analyses. Subsamples of 150 g from each dried sample were dehulled with an impeller husker (model FC2K, Yamamoto Co., Yamagata, Japan) and then milled with a laboratory mill (McGill No. 2, Rapsco, Brookshire, Tex.). The milling duration was 35 s to attain a head rice surface lipid content (SLC) of 0.4%, as measured by near-infrared reflectance (NIR) spectroscopy (DA 7200, Perten Instruments, Springfield, Ill.). After milling, the milled rice was aspirated for 2 min with a seed

blower (South Dakota Seed Blower, Seedboro, Chicago, Ill.) to remove any remaining dust or particles. A laboratory-scale rice sizing device (model 61-117-01, Grainman Machinery Manufacturing, Miami, Fla.) was then used for separating broken kernels from head rice. The head rice obtained after sizing was sorted again by hand to separate milled kernels of 3/4 length or greater of whole kernels. To calculate the HRY, the weight of sorted milled whole kernels was divided by the initial weight of the rough rice sample (150 g).

Subsequent analyses (color measurement) were performed on the milled whole kernels. The color of the whole kernels was measured using an image analysis system (WinSEEDLE Pro 2005a, Regent Instruments Inc., Sainte-Foy, Quebec, Canada). The system comprises a scanning bed with a blue background lid, an acrylic tray sample holder (152 mm × 100 mm × 20 mm), and software that is installed on an auxiliary computer. The measurement method involves spreading 100 head rice kernels from each subsample in a thin layer on the acrylic tray sample holder and placing the sample holder on the scanning bed. The software measures the projected area and quantifies the color of the kernels. The software was calibrated with discolored kernels of interest from this study. The specific colors in the profile were selected and defined as follows: translucent white, opaque white, three shades of yellow, black/brown, red/brown, pink/red, and light pink. The software reports the area of each color classification, and then the percentage of discoloration is calculated as the colored area divided by total projected area.

The microbial isolation and counting processes were performed following the AOAC Method 997.02 (AOAC, 2002). This method involves mixing a 10 g sample of rough rice with 90 mL of sterilized phosphate-buffered dilution water in a sterile stomacher bag and masticating at 0.5 stoke s^{-1} for 240 s. The pulverized samples were used for total microbial load analyses. Consecutive dilutions were made by mixing 1 mL of the mixture with 9 mL of phosphate-buffered dilution

water in a test tube. The dilution was repeated until a 10^{-5} dilution was achieved. Petrifilm mold count plates (3M Microbiology Products, Minneapolis, Minn.) were used for enumeration of mold count. Before enumeration, the inoculated plates were placed in an incubator (Thelco model 4, Precision Scientific Instruments, Inc., Chicago, Ill.) at 25°C for 120 h. After removing the inoculated plates from the incubator, the total colony forming units per gram of rice (CFU g^{-1}) were determined by dividing the enumerated CFU on the plate per gram of rough rice, considering the dilution rate.

2.3.3 Statistical Analysis

First, three-way analysis of variance (ANOVA) was used to determine whether the three treatment factors (MC, temperature, and storage duration) led to any significant changes in discoloration, mold population, and HRY. A total of 240 rice samples from each plot (fungicide and non-fungicide) were randomly assigned to treatment combinations (4 MC levels × 5 temperature levels × 6 weeks × 2 replications). Several ANOVA models were analyzed to confirm the treatment effect with or without interaction terms under the blocking variable (fungicide application). The overall F-test revealed significant treatment effects for all three factors. Note that ANOVA only identifies treatment effects by mean differences, not the effective level of treatment on the response.

Second, we focused on determining the storage conditions, i.e., the levels of MC, temperature, and storage duration, that exhibited the best outcomes for discoloration, mold population, and HRY using response surface methodology (RSM). RSM is basically a second-order polynomial regression in which the treatment factors were treated as continuous explanatory variables with transformation. Due to the significant interaction effects in the preceding models, we stratified the models by week and by temperature. The final models were based on a two-factor standard RSM model, which is also commonly used for central-composite or Box-Behnken designs (Box and

Behnken, 1960). Model diagnostics, such as the assumptions of equal variance, normality, and lack-of-fit test, were performed as appropriate. All analyses were conducted using SAS version 9.4 (SAS Institute Inc., Cary, N.C.) and R version 3.3.2 (R Core Team, Vienna, Austria).

2.4 Results and Discussion

2.4.1 Discoloration Model

The overall regression model for discoloration is as follows:

$$\ln(discoloration) = block_j + MC_j + weeks_j + temp_j + temp_j^2 + MC_j \times weeks_j + MC_j \times temp_j + temp_j \times weeks_j + MC_j \times weeks_j \times temp_j + \varepsilon_j \quad \text{Eq 2.1}$$

where j = 1, …, 240 (index of samples = 4 MC levels × 5 temperature levels × 6 weeks × 2 replications). The block term in the first line of Eq 2.1 indicates the condition of either pre-harvest fungicide or non-fungicide treatment of rice in the field. The main effects of MC, weeks, and temperature and the second-order effect of temperature are in the second line of Eq 2.1. Two-way and three-way interaction terms are in the third and fourth lines, respectively. Finally, the error term (εj) is assumed to be normal, with zero mean and a constant variance. The ln(discoloration) term is the natural logarithm of discoloration. A natural logarithm of discoloration was necessary to fix the nonlinearity and skewness of the data, and the predictors were transformed for orthogonality in RSM.

Each term in Eq 2.1 was worth adding to the model based on the sequential F-test. The quadratic effect of temperature was shown to be significant, indicating a non-linear relationship between

temperature and ln(discoloration). The three-way interactions term among MC, weeks, and temperature was also statistically significant ($p < 0.05$). Any main effect or two-way interaction term cannot be interpreted in a universal way. Therefore, we stratified the regression models by temperature and by weeks to investigate these relationships under certain conditions.

2.4.2 Discoloration Models Stratified by Weeks

Due to the interaction effect, models separated by weeks are proposed here to verify the effects of MC and temperature and their interaction. The six models stratified by weeks are given by:

$$\ln(discoloration)_{ij} = block_{ij} + temp_{ij} + MC_{ij} + MC_{ij} \times temp_{ij} + temp_{ij}^2 + \varepsilon_{ij} \quad \text{Eq 2.2}$$

where j = 1, …, 40 (index of samples = 4 MC levels × 5 temperature levels × 2 replications) for i = 1, 2, …, 6 (index of weeks).

The mean and standard deviation (SD) of discoloration (%) at week 0 were 8.75 and 0.96, respectively. As the storage duration increased, not surprisingly, the mean and SD of discoloration also increased (Table 2.1). The difference in discoloration became evident after six weeks of storage and is attributed to MC, linear and quadratic effects of temperature, and interaction between MC and temperature. The coefficients and p-values were adjusted after controlling for fungicide and non-fungicide treatment effects.

The first-order and second-order terms of temperature indicated a nonlinear relationship between temperature and ln(*discoloration*). MC was positively associated with ln(*discoloration*), but the degree of impact may change with temperature because the interaction term was significant as well. Note that the meaning of a coefficient is not straightforward due to the variable transformations. Therefore, the coefficient was less important because the main objective was to develop a prediction model and ultimately determine the optimal operating conditions. The interaction between temperature and MC was significant, which means that the effect of MC

depends on temperature, and vice versa. In addition, this interaction effect may not be the same in different weeks (very significant after week 6), indicating three-way interaction, as shown in the full model (eq. 2). The R^2 values were reasonably high for prediction purposes after week 6. In the last column of table 1, a higher p-value ($p > 0.05$) indicates no lack-of-fit problem from the F-test. From the coefficients and the model fit, only three models (for weeks 6, 8, and 10) were useful for further prediction and are indicated as (A), (B), and (C) in Table 2.1 and Table 2.3.

Table 2.1 Discoloration change by storage duration (weeks) and affecting factors for long-grain rice hybrid XL745 (MC = moisture content, SD = standard deviation, and temp = storage temperature).

Discoloration (%)			Coefficients[a]				Model Fit	
Weeks	Mean	SD	Temp	MC	MC × Temp	$Temp^2$	R^2	Lack of Fit
2	9.11	1.62	0.11**	-0.05	0.08*	0.03	0.54	0.10
4	9.21	3.20	0.18*	0.14*	0.13	0.01	0.31	0.99
(A) 6	12.87	9.19	0.32***	0.14**	0.23**	0.25**	0.73	0.45
(B) 8	15.17	15.05	0.43***	0.26 ***	0.41***	0.47***	0.89	0.70
(C) 10	17.03	19.51	0.59***	0.26 ***	0.37 ***	0.58***	0.93	0.55
12	19.19	23.00	0.63***	0.21***	0.38***	0.59***	0.91	0.005

[a] Asterisks indicate p-values: * = $p < 0.05$, ** = $p < 0.01$, and *** = $p < 0.001$.

Figure 2.1 shows contour plots of the response surface for the interaction effect of MC and storage temperature on the response of ln(*discoloration*). Due to the natural logarithm scale of the response, 4 is equivalent to 55% discoloration, 3 is about 20%, and 2.3 is about 10%. Both high MC and high temperature (top right corners of the contour plots) had the most severe effect on discoloration, although the degree of severity depended on the storage duration (weeks). Meanwhile, lower levels of the mean response were associated with either lower temperature or lower MC. The yellow highlighted areas indicate the safe storage zones, i.e., optimal MC and temperature conditions to maintain about 10% discoloration, which is close to the control conditions.

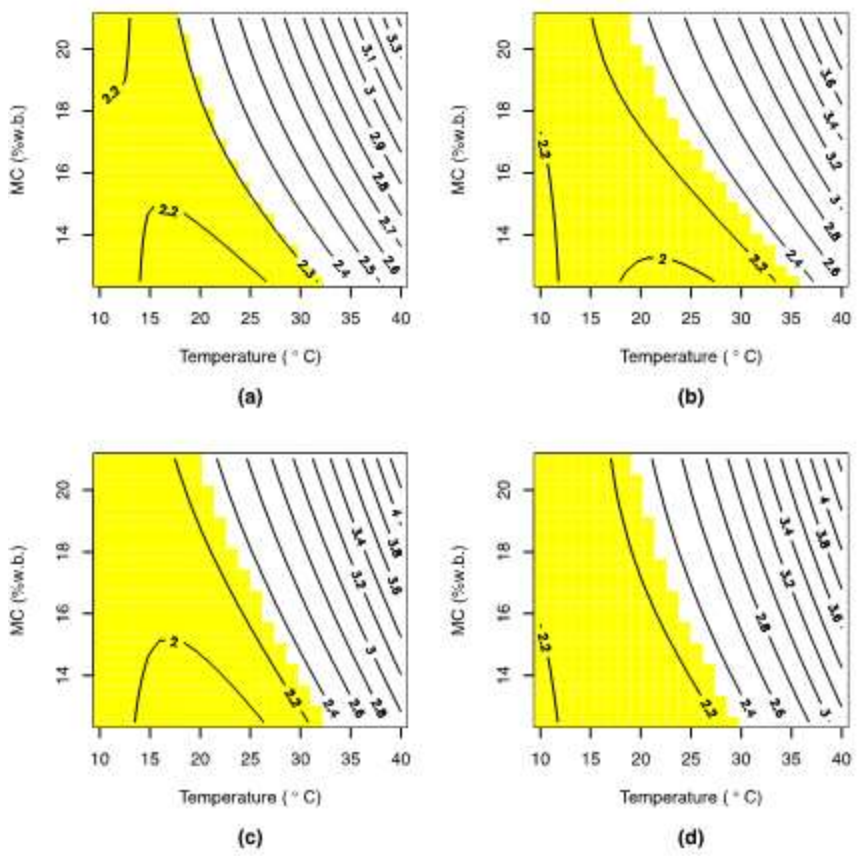

Figure 2.1 Contour plots of response surface of ln(*discoloration*) for MC and temperature at different weeks of storage for long-grain rice hybrid XL745: (a) week 6, (b) week 8, (c) week 10, and (d) week 12 (MC = moisture content, and w.b. = wet basis).

2.4.3 Discoloration Models Stratified by Temperature

Separating the models by temperature allowed us to focus on MC, weeks, and their interaction at a given temperature. The five models stratified by temperature are given by:

$$\ln(discoloration)_{ij} = block_{ij} + weeks_{ij} + MC_{ij} + MC_{ij} \times weeks_{ij} + \varepsilon_{ij} \quad \text{Eq 2.3}$$

where j = 1, …, 48 (index of samples = 4 MC levels × 6 weeks × 2 replications) for i = 1, 2, …, 5 (index of temperature levels).

Table 2.2 summarizes the results of the discoloration change by temperature and other affecting factors. From the coefficients and the model fit, only one temperature model (40°C) was useful for further prediction and is indicated as (D) in Table 2.2 and

Table 2.4.

Table 2.2 Discoloration change by storage temperature (temp) and affecting factors for long-grain rice hybrid XL745 (MC = moisture content, SD = standard deviation, and weeks = storage duration).

Discoloration (%)			Coefficients[a]			Model Fit	
Temp (°C)	Mean	SD	Weeks	MC	Weeks × MC	R^2	Lack of Fit
10	8.20	1.53	0.02	0.01	0.05	0.06	0.48
15	9.13	1.81	-0.01	-0.03	0.07	0.08	0.48
20	9.21	2.18	0.04	0.12**	-0.001	0.24	0.53
27	10.66	3.51	0.12*	0.18***	0.15*	0.51	0.91
(D) 40	31.60	25.77	0.85***	0.52***	0.38***	0.88	0.21

[a] Asterisks indicate p-values: * = $p < 0.05$, ** = $p < 0.01$, and *** = $p < 0.001$.

The interaction effect between MC and weeks (storage duration) was shown to be significant at 27°C and 40°C. Longer storage with higher MC jointly affected the discoloration, especially at high temperatures. Figure 2.2 shows contour plots of the response surface for the mean levels of ln(*discoloration*), storage duration, and MC. Due to the natural logarithm scale of the response, 4.6 is equivalent to about 99% discoloration, 3 is about 20%, and 2.3 is about 10%. Both long storage duration and high MC (top right corners of the contour plots) had the most severe response for discoloration, especially at 40°C. Lower levels of mean response are associated with either lower MC or shorter storage duration. The yellow highlighted areas indicate the safe storage zones with optimal conditions of MC and storage duration to maintain 10% or less discoloration.

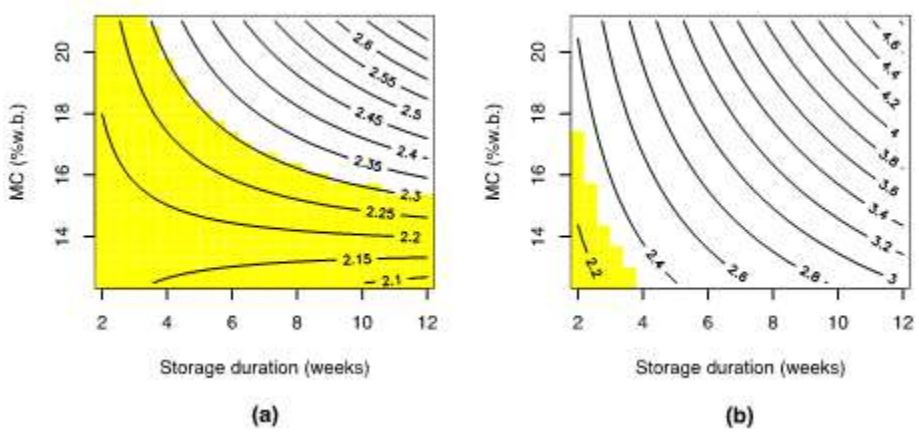

Figure 2.2 Contour plots of response surface of ln(*discoloration*) for MC and storage duration at different temperatures for long-grain rice hybrid XL745: (a) 27°C and (b) 40°C (MC = moisture content, and w.b. = wet basis).

2.4.4 Week 0 versus Week 2

The initial condition of discoloration at week 0 was not included in the regression analysis because the environmental conditions at week 0, such as temperature, were independent of the experimental conditions during the following 12 weeks. Therefore, our measurements began at week 2. Separate analyses were conducted and compared between week 0 and week 2. After controlling MC and fungicide treatment (block effect), there was no significant difference in discoloration between week 2 and week 0. Therefore, it is reasonable to assume that the discoloration at week 2 represented the initial condition of storage.

2.4.5 Model Prediction

Response surface models provide optimal operating conditions and can also be used for prediction. From the model evaluation (R^2 and lack-of-fit test) in tables 1 and 2, the four models (A), (B), (C), and (D) were applied to predict the expected ln(*discoloration*). In Table 2.3, the predicted conditions of discoloration are summarized after week 6, week 8, and week 10 at 20% MC and 35°C in storage. For example, using model (C) in Table 2.2, the discoloration at week 10 can be estimated with predictors of the initial MC of 20%, 35°C, and pre-harvest fungicide treatment and is approximately 36% with a confidence interval (CI) of (31, 42). This discoloration is substantial compared to the initial discoloration of 9%.

Our proposed models were stratified based on weeks and based on temperature, so we used a different model with 40°C as a predictor (

Table 2.4). For example, at 40°C, the expected discoloration level is approximately 47% with CI (40, 55) for 20% MC and nine weeks of storage for the non-fungicide treatment group. The fungicide group showed a higher level of discoloration, about 56%, with the same predictors. In another example, about 8.5 weeks on average (CI: 5.8, 11.1) were required for the fungicide

treatment group to reach 50% discoloration, whereas about 9.3 weeks (CI: 6.7, 12) were required for the non-fungicide treatment group.

Table 2.3 Expected discoloration at 20% MC and 35°C by weeks of storage for long-grain rice hybrid XL745 (L95 and U95 are the lower and upper bounds, respectively, of the 95% confidence interval).

	Fungicide			Non-Fungicide		
Weeks	Discoloration (%)	L95	U95	Discoloration (%)	L95	U95
(A) 6	21.18	17.74	25.29	18.68	15.64	22.30
(B) 8	31.27	26.64	36.72	25.81	21.99	30.31
(C) 10	35.80	30.88	41.51	30.46	26.27	34.65

Table 2.4 Expected discoloration at 20% MC, nine weeks of storage, and 40°C for long-grain rice hybrid XL745 (L95 and U95 are the lower and upper bounds, respectively, of the 95% confidence interval).

Temperature	Fungicide			Non-Fungicide		
(°C)	Discoloration (%)	L95	U95	Discoloration (%)	L95	U95
(D) 40	56.42	48.53	65.60	46.87	40.31	54.49

2.4.6 Mold Count Stratified by Weeks

Second-order polynomial regressions of mold count stratified by weeks are given by:

$$Mold\ count_{ij} = block_{ij} + temp_{ij} + MC_{ij} + MC_{ij} \times temp_{ij} + temp_{ij}^2 + MC_{ij}^2 + \varepsilon_{ij} \quad \text{Eq 2.4}$$

where $j = 1, \ldots, 40$ (index of samples = 4 MC levels × 5 temperature levels × 2 replications) for $i = 1, 2, \ldots, 6$ (index of weeks).

In Table 2.5, the mean values of mold count substantially increased at 8 weeks of storage but then slightly decreased after weeks 10 and 12. However, the overall mean value of mold count did not increase during the experiment compared to the value at 0 weeks (5.92 ±0.09). There was a significant difference in mold count between week 0 and week 2 in the separate analysis. During the experiment (weeks 2 to 12), the variation in mold count at a fixed week can be explained by temperature, MC, and their quadratic effects, although the interaction effect was minor.

Rice encounters molds of two general classifications: field fungi and storage fungi. Predominant field fungi include species of *Fusarium*, while predominate storage fungi include species of *Aspergillus*. It is expected that the general growth responses of molds, in terms of populations at the studied conditions, would be similar. Other studies have documented that kernels may have unique stains in isolated cases when the crop is heavily affected in the field with some types of mold (Schroeder, 1965). Microorganisms may grow across a wide range of temperatures: mesophiles grow at moderate temperatures (20°C to 45°C), psychrophiles can live at much lower temperatures (-20°C to +10°C, and thermophiles thrive at relatively high temperature (60°C to 108°C). The minimum equilibrium relative humidity (%ERH) value for microbial growth is 60%. Molds are aerobic organisms and do not grow well in conditions where oxygen is limited. In this study, sealed (anaerobic) conditions were used for storage.

Figure 2.3 shows contour plots of the response surface for mold count. The pink highlighted areas indicate where the mold level did not change from the initial level (week 0). Therefore, the previous results for the optimal conditions for discoloration remained the same under the assumption of restrained mold population. Higher levels of mold population are associated with higher MC and lower temperature (top left corners of the contour plots). The minimum mold population is achieved at either a high temperature or a low MC (<16%).

Table 2.5 Mold count (log_{10} CFU g^{-1}) change by storage duration (weeks) and affecting factors for long-grain rice hybrid XL745 (MC = moisture content, SD = standard deviation, and temp = storage temperature).

Mold Count (log_{10} CFU g^{-1})			Coefficients[a]					Model Fit	
Weeks	Mean	SD	Temp	MC	MC × Temp	$Temp^2$	MC^2	R^2	Lack of Fit
2	5.17	0.86	-0.49*	-0.33	0.003	-0.09	0.11	0.30	0.39
4	4.96	0.90	-0.71***	-0.55***	-0.35*	-0.42*	-0.18	0.75	0.89
6	5.15	1.07	-0.86***	0.10	-0.28	-0.80***	0.61**	0.79	0.57
8	5.77	0.85	-0.40*	0.47**	0.10	-0.42	0.84**	0.52	0.62
10	5.64	0.86	-0.56**	0.41**	0.06	-0.47*	0.46*	0.59	0.60
12	5.41	0.99	-0.72***	0.63***	0.32*	-0.58**	0.67**	0.79	0.04

[a] Asterisks indicate p-values: * = $p < 0.05$, ** = $p < 0.01$, and *** = $p < 0.001$. Coefficients and p-values are adjusted for block (fungicide/non-fungicide)

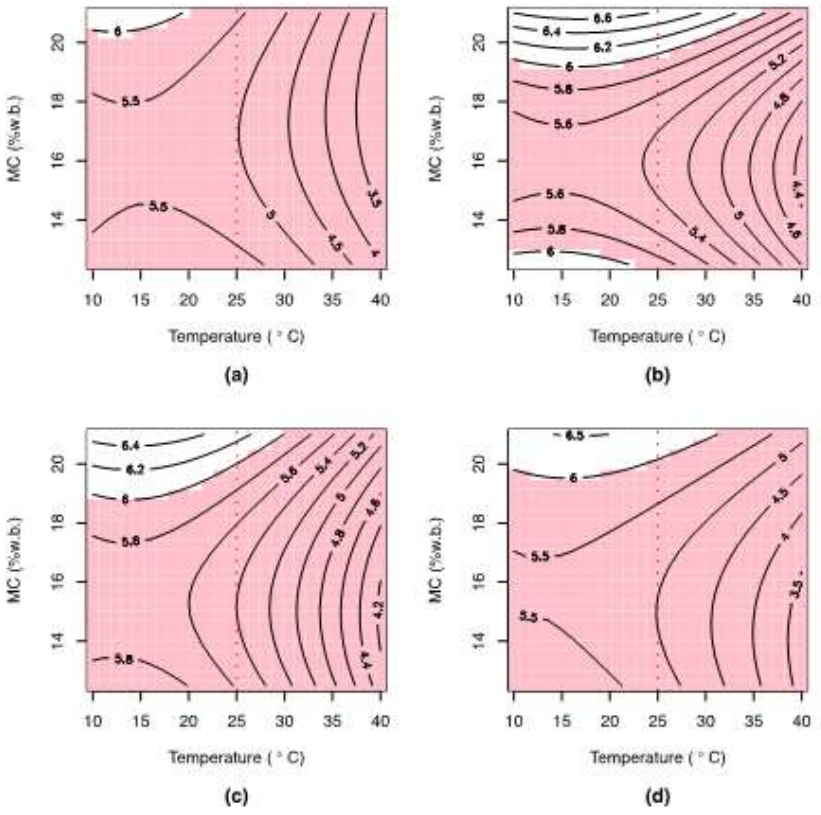

Figure 2.3 Contour plots of response surface of mold count (log_{10} CFU g^{-1}) for MC and temperature at different weeks of storage for long-grain rice hybrid XL745: (a) week 6, (b) week 8, (c) week 10, and (d) week 12 (MC = moisture content, and w.b. = wet basis).

2.4.7 Mold Count Models Stratified by Temperature

Five models stratified by temperature are given by:

Eq 2.5

$$Mold\ count_{ij} = block_{ij} + weeks_{ij} + MC_{ij}$$

$$+MC_{ij} \times weeks_{ij} + weeks_{ij}^2 + MC_{ij}^2 + \varepsilon_{ij}$$

where j = 1, …, 48 (index of samples = 4 MC levels × 6 weeks × 2 replications) for i = 1, 2, …, 5 (index of temperature levels).

In Table 2.6, the mean values of mold count decreased as temperature increased. The variation in mold count at a fixed temperature can be explained by weeks, MC, and their interaction. Based on the significant coefficients and overall average mold population, the result at 40°C can be separated from the results at lower temperatures.

In Figure 2.4, at 20°C, the interaction term between storage duration (weeks) and MC is significant. Therefore, the effect of storage duration (weeks) or MC cannot be interpreted in a universal way. The mold population grew slowly as storage duration increased at high MC (20%); however, this was not true for lower MC. Similar analyses were performed for storage at 10°C, 15°C, and 27°C. MC does not behave singularly but rather affects mold count jointly with temperature. At low temperatures, high MC is associated with mold population over time at either a linear rate or a nonlinear (slow) rate.

The low MC effect is not clear over time at low temperature. The overall mean mold population was lower for samples stored at 40°C (Figure 2.4b) than for samples stored at 20°C (Figure 2.4a). The lower mold count at higher storage temperature could have been due to the lack of oxygen available for mold population in the anaerobic storage conditions (Pardo et al., 2004). At high MC (20%), the mold population is positively and linearly associated with storage duration. At low MC

(14%), the mold population is negatively associated with storage duration. At high temperature (40°C), high MC has a negative impact for a long-term storage. Storage at low MC may have a positive impact for a short-term storage by retarding mold population. The form in which rice is stored may also affect storability. The role of the husk in protecting the grain against microbial attack at suboptimal MC and temperature conditions has been reported (Liu et al., 2006). In our experiment, paddy rice was kept in airtight storage, which also contributed to inhibiting mold development.

Table 2.6 Mold count (log_{10} CFU g^{-1}) change by storage temperature (temp) and affecting factors for long-grain rice hybrid XL745 (MC = moisture content, SD = standard deviation, and weeks = weeks of storage).

Mold Count (log_{10} CFU g^{-1})			Coefficients[a]					Model Fit	
Temp (°C)	Mean	SD	Weeks	MC	Weeks × MC	$Weeks^2$	MC^2	R^2	Lack of Fit
10	5.80	0.36	0.26***	0.12*	0.25**	-0.07	0.20*	0.50	0.001
15	5.75	0.44	0.29***	0.16*	0.38***	-0.23*	0.25*	0.561	0.12
20	5.61	0.74	0.38**	-0.004	0.60**	-0.46*	0.10	0.38	0.38
27	5.40	0.63	0.31**	0.02	0.49**	-0.09	0.34	0.37	0.23
40	4.18	1.26	0.11	0.31	0.78*	0.08	1.21**	0.29	0.18

[a] Asterisks indicate p-values: * = $p < 0.05$, ** = $p < 0.01$, and *** = $p < 0.001$.

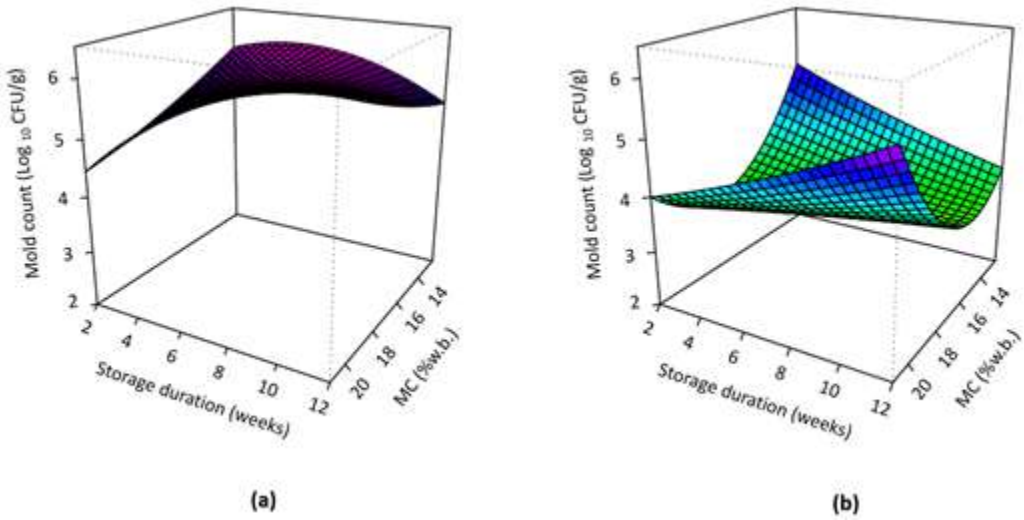

Figure 2.4 Mold count (log_{10} CFU g^{-1}) versus grid of storage duration (weeks) and MC at different temperatures for long-grain rice hybrid XL745: (a) 20°C and (b) 40°C (MC = moisture content, w.b. = wet basis, and CFU = colony forming units).

2.4.8 Head Rice Yield Model

Six HRY models stratified by weeks are given by:

$$Head\ rice\ yield_{ij} = block_{ij} + temp_{ij} + MC_{ij} + MC_{ij} \times temp_{ij} + MC_{ij}^2 + \varepsilon_{ij} \quad \text{Eq 2.6}$$

where j = 1, …, 40 (index of samples = 4 MC levels × 5 temperature levels × 2 replications) for i = 1, 2, …, 6 (index of weeks).

In Table 2.7, there is some evidence of the effect of MC and temperature on HRY, but with no regular pattern. The overall variations of the mean and SD over 12 weeks were not substantial in this experiment. It is not clear what factor is important over the storage duration. Based on Figure 2.5, the green areas are relatively better zones that maintained the HRY as that of the initial sample. There was a significant negative interaction effect between MC and temperature, which caused a greater reduction in HRY. However, this interaction effect no longer existed at weeks 8, 10, or 12. Models stratified by temperature were also analyzed, and the results showed lack of fit, poor R^2 and no meaningful interpretation.

Table 2.7 Head rice yield (HRY, %) change by storage duration (weeks) and affecting factors for long-grain rice hybrid XL745 (MC = moisture content, SD = standard deviation, and temp = storage temperature).

HRY (%)			Coefficients[a]				Model Fit	
Weeks	Mean	SD	Temp	MC	MC × Temp	MC^2	R^2	Lack of Fit
2	50.26	1.48	-0.29	-1.36***	0.10	-0.63	0.66	0.94
4	50.48	1.76	-1.21***	-1.08***	-0.86**	-0.54	0.71	0.68
6	50.86	1.03	-0.80***	-0.38*	-0.48*	-0.41	0.63	0.03
8	51.01	1.46	-0.65**	0.31	-0.04	-1.05**	0.73	0.72
10	49.09	1.19	-0.36	0.48	0.18	-0.43	0.28	0.49
12	49.06	1.34	-0.53*	-0.56**	-0.26	1.27***	0.62	0.01

[a] Asterisks indicate p-values: * = $p < 0.05$, ** = $p < 0.01$, and *** = $p < 0.001$.

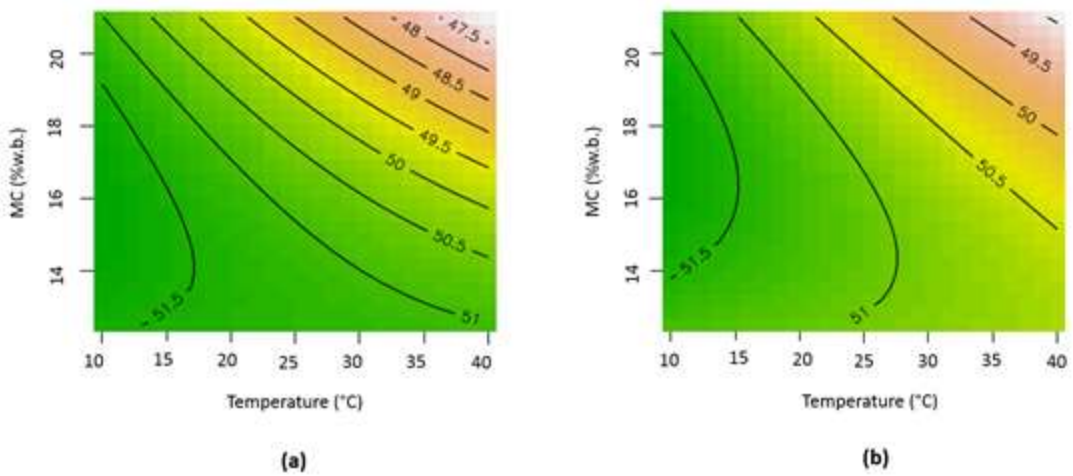

Figure 2.5 Contour plot of response surface of head rice yield (%) for hybrid long grain rice (XL745); weeks 4 (a); weeks 6 (b); MC indicates moisture content; w.b. indicates wet basis.

2.4.9 Fungicide versus Non-Fungicide Effect

In this study, fungicide and non-fungicide treatment were considered as a block. Inclusion of this block is meaningful as a control variable to improve the precision of the estimation of other treatment effects. To test the fungicide and non-fungicide treatment effect, a Mann-Whitney test was conducted; this test is often viewed as an alternative nonparametric version of a two-sample t-test. A Mann-Whitney test is performed to determine if two independent samples are from the same distribution. A small p-value ($p < 0.05$) indicates a difference between the two samples. In Figure 2.6, fungicide treatment significantly improved the HRY but also slightly increased ln(*discoloration*) and mold count, indicating some trade-off in rice quality. It can be speculated that field fungicide treatment inhibited field fungi activity, which subsequently preserved the rice bran layer. Improved integrity of the bran could significant increase the HRY of samples from fields with fungicide treatment.

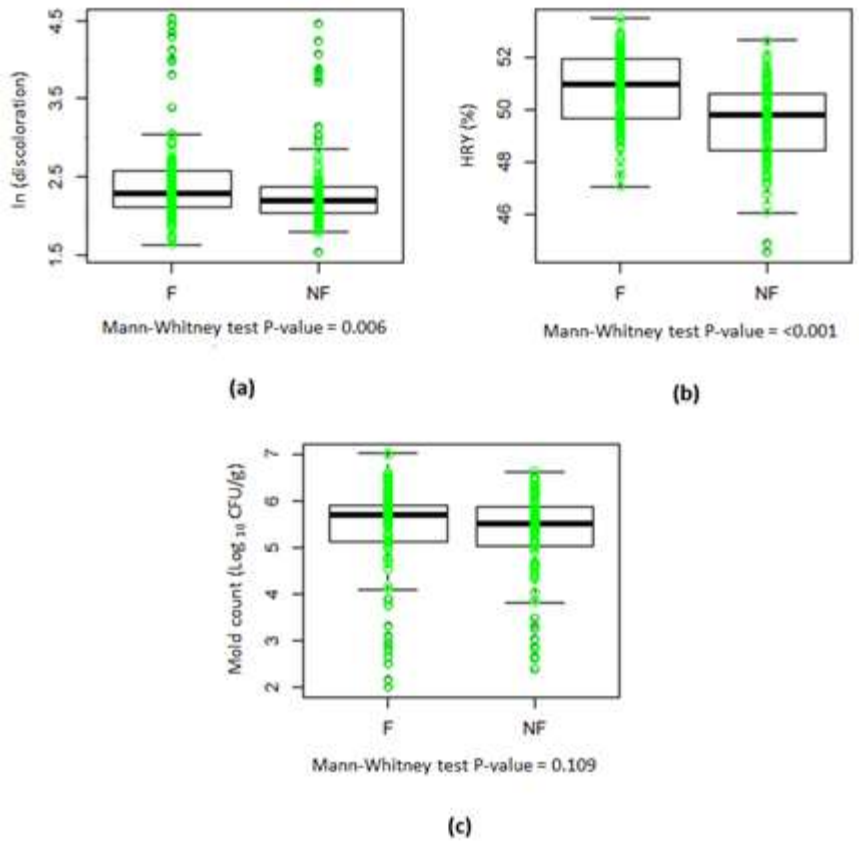

Figure 2.6 Impacts of pre-harvest fungicide treatment of long-grain rice hybrid XL745 on rice quality characteristics: (a) ln(*discoloration*), (b) HRY (%), and (c) mold count (log_{10} CFU g^{-1}) (CFU = colony forming units, F = fungicide treatment, and NF = non-fungicide treatment).

2.5 Conclusion

This study documented safe storage conditions for rough rice to mitigate the negative effects of HRY reduction, mold population, and discoloration. There was a quadratic effect of MC on rice quality. Higher MC tended to increase both discoloration and mold population, lowering the quality of the rice, although this effect may change with temperature or storage duration. High temperature tended to increase discoloration but may suppress the mold population (conflicted effect of temperature) in anaerobic conditions. According to the regression model, the critical storage temperature that may lead to discoloration is between 27°C and 40°C. From the contour plots for storage durations of 6 to 12 weeks, the minimum mold population is achieved at high temperature (40°C). However, this result could have been due to inactivation of molds at high

temperature and in sealed (anaerobic) storage conditions. The variations in mold population can be explained by the effects of MC and temperature and their quadratic effects. When the temperature level was fixed (e.g., less than 25°C), then samples stored with average MC of 16% tended to have minimum mold populations.

Data showed that the quality of long-grain hybrid rice can be optimized by carefully controlling storage MC, temperature, and duration. Optimizing parameters such as rough rice storage MC as a function of the predicted storage duration would help optimize the quality of U.S. rice destined to the consumer or processing markets. Considering pre-harvest rice management, there may be a need to increase the application rate of conventional fungicide (>17 oz. per acre), adjust the application timing, or change the type of fungicide used if a significant impact on post-harvest rice quality, specifically HRY, is to be expected.

Acknowledgement

The authors acknowledge the University of Arkansas' Division of Agriculture and the Rice and Grain Processing program for collaboration and providing facilities. This study was based on work that is supported, in part, by USDA National Institute of Food and Agriculture Hatch Act funding.

2.6 References

AAOC. (2002). Official method 997.02: Yeast and mold counts in foods. Rockville, MD: Association of Official Agricultural Chemists.

ASABE (2017). S352.2: Moisture measurement - Unground grain and seeds. St. Joseph, MI: ASABE.

Atungulu, G. G., Thote, S., & Wilson, S. (2016). Storage of hybrid rough rice: Consideration of microbial growth kinetics and prediction models. *J. Stored Prod. Res., 69*, 235-244.

Bason, M. L., Gras, P. W., Banks, H. J., & Esteves, L. A. (1990). A quantitative study of the influence of temperature, water activity, and storage atmosphere on the yellowing of paddy endosperm. *J. Cereal Sci., 12*(2), 193-201.

Box, G. E., & Behnken, D. W. (1960). Simplex-sum designs: A class of second-order rotatable

designs derivable from those of first order. *Ann. Math. Stat., 31*(4), 838-864.

Cooper, N. T., Siebenmorgen, T. J., Counce, P. A., & Meullenet, J.-F. (2006). Explaining rice milling quality variation using historical weather data analysis. *Cereal Chem., 83*(4), 447-450.

Debabandya, M., & Satish, B. (2004). Wear of rice in an abrasive milling operation, Part II: Prediction of bulk temperature rise. *Biosyst. Eng., 89*(1), 101-108.

Dong, Y., Tsuzuki, E., Lin, D., Kamiunten, H., Terao, H., Matsuo, M., & Cheng, S. (2003). Molecular genetic mapping of quantitative trait loci for milling quality in rice (*Oryza sativa* L.). *J. Cereal Sci., 40*(2), 109-114.

Ghadge, P. N., & Prasad, K. (2012). Some physical properties of rice kernel: Variety PR-106. *J. Food. Proc. Tech., 3*(8), 1-5.

Kim, H., Kim, O.-W., Kwak, H. S., Kim, S. S., & Lee, H.-J. (2017). Prediction model of rice eating quality using physicochemical properties and sensory quality evaluation. *J. Sensory Studies, 32*(4), e12273.

Liu, Z., Gao, J., & Yu, J. (2006). Aflatoxins in stored maize and rice grains in Liaoning province, China. *J. Stored Prod. Res., 42*(4), 468-479.

Marchezan, E. (1991). Graos inteiros em arroz (Whole rice kernels in rice). *Lavoura Arrozeira, 44*, 3-8.

Mason, L. J., Rulon, R. A., & Maier, D. E. (1997). Chilled versus ambient aeration and fumigation of stored popcorn, part 2: Pest management. *J. Stored Prod. Res., 33*(1), 51-58.

Meullenet, J.-F., Marks, B. P., Hankins, J.-A., Griffin, V. K., & Daniels, M. J. (2000). Sensory quality of cooked long-grain rice as affected by rough rice moisture content, storage temperature, and storage duration. *Cereal Chem., 77*(2), 259-263.

Neninger, L. H., Hidalgo, E. I., Barrios, L. M., & Pueyo, M. (2003). Hongos presentes en semillas de arroz (*Oryza sativa* L.) en Cuba. *Fitosanidad, La Habana, 7*, 7-11.

Pardo, E., Marin, S., Sanchis, V., & Ramos, A. J. (2004). Prediction of fungal growth and ochratoxin A production by *Aspergillus ochraceus* on irradiated barley grain as influenced by temperature and water activity. *Intl. J. Food Microbiol., 95*(1), 79-88.

Pinciroli, M., Gribaldo, A., Vidal, A., Bezus, R., & Sisterna, M. (2013). Mycobiota evolution during storage of paddy, brown, and milled rice in different genotypes. *Summa Phytopathologica, 39*(3), 157-161.

Rehal, J., Kaur, G. J., & Singh, A. K. (2017). Influence of milling parameters on head rice recovery: A review. *Intl. J. Curr. Microbiol. App. Sci., 6*(10), 1278-1295.

Sajawan, K. S., Laplan, D. I., Mittra, B. N., & Pandey, H. K. (1990). Influence of the post-harvest

operations on the milling quality of rice. *Intl. J. Trop. Agric., 8*, 304-309.

Schroeder, H. W. (1965). Fungus deterioration of rice: Effects of fungus infection on free amino acids and reducing sugars in white and par-boiled rice. *Cereal. Chem., 42*, 539-545.

Shafiekhani, S., Wilson, S. A., & Atungulu, G. G. (2018). Impacts of storage temperature and rice moisture content on color characteristics of rice from fields with different disease management practices. *J. Stored Prod. Res., 78*, 89-97.

Siebenmorgen, T. J., Counce, P. A., Lu, R., & Kocher, M. F. (1992). Correlation of head rice yield with individual kernel moisture content distribution at harvest. *Trans. ASAE, 35*(6), 1879-1884.

Siebenmorgen, T. J., Grigg, B. C., & Lanning, S. B. (2013). Impacts of preharvest factors during kernel development on rice quality and functionality. *Ann. Rev. Food Sci. Tech., 4*(1), 101-115.

Trigo-Stockli, D. M., & Pedersen, J. R. (1994). Effect of rice storage conditions on the quality of milled rice. *Proc. 6th Intl. Conf. Stored Product Protection* (vol. 2, pp. 706-711). Wallingford, UK: CABI.

USDA. (2009). United States Standards for rice. Washington, DC: Federal Grain Inspection Service.

USDA. (2018). Commodity loan rates. Washington, DC: USDA.

Vincent, C., Weintraub, P. G., Hallman, G. J., & Fleurat-Lessard, F. (2008). Insect management with physical methods in pre- and post-harvest situations. In E. B. Radcliffe, R. E. Cancelado, & W. D. Hutchison (Eds.), *Integrated pest management: Concepts, tactics, strategies, and case studies* (pp. 309-323). Cambridge, UK: Cambridge University Press.

Chapter 3: **Effect of rice chilling on drying, milling and quality characteristics**

Soraya Shafiekhani, Griffiths G. Atungulu

3.1 Abstract

High temperature (field heat) and moisture content of freshly harvested rough rice promote excessive respiration and microbial growth. Therefore, the rice risks significant deterioration of quality due to delayed drying at peak harvest time when drying capacity becomes limited. The U.S. rice industry has identified that cooling/chilling the rice prior to drying to remove the excess heat, immediately after harvest, significantly preserves the quality of milled rice. This study experimentally simulated drying of rough rice after cold storage/chilling. The rice was dried using slightly-heated air and high temperature air with procedures set to mimic those practiced by commercial systems. Rough rice at moisture contents (MCs) of 16%, 19%, and 21% (wet basis) were stored at storage temperature (T_s) of 10°C, 15°C, and 20°C for up to 4 months. Following retrieval, the samples were dried at drying temperature (T_d) of 35°C, 45°C, and 60°C and relative humidity (RH) of 20%. Each drying run comprised of two 20-min drying passes with the rice tempered at the drying T_d for a duration of 4 h following every drying pass. Following the drying, the rice was conditioned in an equilibrium MC chamber (T=26°C, RH=56%) to 12.5% MC and then milled to evaluate milled rice yield and quality characteristics. The highest percentage points of MC removal (6.77 % points) occurred following drying at air temperature of 60°C for samples with initial MC at 21% and stored at 20°C. Drying with air at 60°C decreased head rice yield (HRY) especially for samples with initial MC at 21% and stored at 10°C (HRY=51.4% versus those at 45°C and 35°C, HRY=55.95% and HRY=58.8%, respectively). Drying air temperatures studied (35°C, 45°C, 60°C) had no significant effect of causing discoloration of samples within the range of the studied initial MCs and storage temperatures. Peak and final viscosities of samples

with different initial MCs (16%, 19% and 21%) stored at 20°C followed by high temperature air drying (60°C) were significantly different from those of samples stored at 10°C and 15°C. The results provided insight into the drying, milling and quality characteristics of rice after cold storage/chilling. The information provide foundation for development of new recommendations to improve quality of milled rice.

Keywords: Rough rice, Cooling/chilling, Conventional drying, Storage, Milling quality.

3.2 Introduction

Rough rice chilling is accomplished by cooling of the grain to below ambient temperature using a mechanical refrigeration system (Brunner, 1990). First, the application of rice chilling may permit both short- and long-term storage of the grain regardless of the ambient conditions. Pre-chilling the grain before drying may help producers overcome drying capacity related pressure during peak harvest time (Maier et al., 1992). Secondly, chilling of rough rice followed by storage provides the opportunity to store the grain safely without using chemical protectant for insect pest control (Thorpe and Elder, 1982; Navarro and Noyes, 2002). Third, improvement of rice milling quality has also been reported for grain stored in chilled environment (Rius, 1987; Shafiekhani and Atungulu, 2017; Shafiekhani et al., 2018; Shafiekhani et al., 2019; Atungulu and Shafiekhani, 2019). Maier et al. (1992) reported a market price of $16/cwt for milled parboiled rice which makes the chilled-aeration storage an attractive technology for both the quality preservation of stored rough rice and the conditioning of parboiled rice.

A rice kernel can be regarded as a composite material consisting of several different biopolymers, including starch and proteins with moisture as a plasticizer (Meesukchaosumran and Chitsomboon, 2018; Luthra et al., 2019; Shafiekhani et al., 2016). At low temperatures or moisture contents, starch granules in rice behave as a glassy material. Addition of thermal energy into the rice initiates

movement of starch granules and phase change which cause the starch to display rubbery or flexible characteristics (Ondier et al., 2012; Amiri et al., 2019; Anari et al., 2019). In the first stage of drying, the surface of the rice kernel loses moisture faster than the core of the kernel; this makes the rice surface to transition into the glass state first while the core is still in the rubbery state. This state differential may cause compressive stress and fissuring (Yang and Jia, 2004). The effect of moisture content (MC) on the glass transition temperature (T_g) for individual long grain rice kernels was measured using dynamic mechanical thermal analysis; the T_g equation developed by Siebenmorgen et al. (2004) is shown using the following regression equation:

$$Tg = 100.5 - 334 \times MC \quad \text{Eq 3.1}$$

where, T_g is the glass transition temperature (°C), MC is the moisture content, expressed on a decimal wet basis.

Practically, rice growers have the option to chill freshly-harvested high moisture content rough rice and proceed with storage at low temperatures, during peak harvest, and dry later using commercial natural or heated air-drying systems. High temperature air drying of the rough rice requires that multiple passes of air with tempering step be used to minimize fissure formation. Schluterman and Siebenmorgen (2004) reported high milling yields of rice by using drying air temperatures of 40°C to 65°C with multiple passes of 20-40 min for each pass. Combining chilling aeration with high temperature drying of paddy in Malaysia increased drying capacity by 40% (Chek, 1989).

Typically, tempering conditions are designed to reduce or prevent fissuring of the rice kernels. Ondier et al. (2012) reported that the tempering temperature should be the same as the drying air temperature to avoid phase transition from a rubbery to glassy state. Moreover, they considered the sealed headspace condition by using sealed/airtight plastic bags for tempering which minimize

reduction in the rice milling quality. Steffe et al. (1979) suggested that a 3 h tempering duration was sufficient after drying for 20 min using drying air at 50°C.

There is very limited information on the drying behavior of freshly-harvested, high moisture rough rice subjected to cooling or chilling pre-drying and consequence of such practice on the milled rice quality. This study experimentally simulated slightly-heated and high air temperature drying of rough rice subjected to cold storage/chilling; the drying procedures were set to mimic those practiced by commercial drying systems, which use multi-pass drying and tempering. We hypothesized that storage/chilling temperatures prior to drying, and drying air conditions will influence the rough rice drying behavior and quality of milled rice. The objective for the current study was to determine moisture removal, milling and quality characteristics of the rice upon drying with the described drying methods. The results of this study describe the appropriate use of chilling aeration systems in the rice industry.

3.3 Materials and Methods

3.3.1 Collection and Preparation of Samples

Hybrid long-grain rice cultivar (XL745) was harvested in the year 2017 from Pocahontas, Arkansas at MC 22% (wet basis). Henceforth, moisture content (MC) is expressed on a wet basis (w.b.) unless specified otherwise. Rice samples were cleaned with a dockage tester (Model XT4, Carter-Day, Minneapolis, MN). Then, the cleaned rice was divided into three sub lots. The weight of each sub lots was 6 kg. The sub lots were conditioned to obtain samples at MCs of 16%, 19%, and 21% using conditioned environment chamber (5580A, Parameter Generation and Control, Black Mountain, N.C.) set at 26°C and 56% relative humidity (RH). In these conditions drying lasted 24 h to reach a MC of 16%. The MC of the samples was measured following the procedure by the American Society of Agricultural and Biological Engineers (ASABE) Standard S352.2

(ASABE Standards, 2008) which involves putting 15-g of the rough rice in an oven (1370 FM, Sheldon Mfg., Inc., Cornelius, OR) set at 130°C for 24 h. After conditioning, the samples were stored in individual well labeled, sealed glass jars at three separate refrigerators with temperatures of 10°C, 15°C, and 20°C for 4 months. The storage temperatures were chosen based on cool ambient conditions through summer till late-fall season in Arkansas. Prior to drying, samples were withdrawn from storage and allowed to equilibrate to ambient temperature. Two replications were used for each storage conditions.

3.3.2 Drying Air Conditions

Rough rice was taken out from glass jars and was placed on a tarp (thin layer) in controlled environment chamber (ESPEC, Hudsonville, Mich) to dry with different drying air conditions of 35°C, 45°C, and 60°C with constant 20% RH; the drying air conditions correspond to EMCs of 7.33%, 6.64%, and 5.77% respectively as predicted by the modified Chung-Pfost equation for rice. A temperature/relative humidity sensor (Onset Corporation, Bourne, MA, USA; accuracy: ±0.21°C and 2.5% RH) was placed inside the chamber to measure air conditions every 60 s during drying. For each drying condition, samples were dried for two 20-min drying passes. Immediately after each drying run, the rice samples were placed in individual sealed glass containers and tempered for 4 h at the drying air temperature (there were 4-hours tempering periods between each 20-minute drying pass). After tempering, the samples were taken out of the sealed glass containers and placed into an EMC chamber maintained at 26°C and 56% RH to gently dry to 12.5% MC. After each drying run, the actual MC loss of the sample was determined gravimetrically. The MC of the samples was confirmed following the procedure by ASABE Standard S352.2. The moisture removal was calculated as the difference between the initial MC and the final MC after 2nd drying pass and reported as percentage points MC (PPMC) removal.

3.3.3 Milling Analysis

150-g from each dried sample were dehulled with an impeller husker (Model FC2K, Yamamoto, Yamagata, Japan), then milled with a laboratory mill (McGill No. 2, RAPSCO, Brookshire, TX). Rice milling was set to standardize the degree of milling (Cooper and Siebenmorgen, 2007). Milling duration were selected as 35 s to attain a head rice surface lipid content (SLC) of 0.4% as measured by near-infrared reflectance (NIR) spectroscopy (DA 7200, Perten Instruments). After milling, the milled rice was aspirated for 2 min with a seed blower (South Dakota Seed Blower, Seedboro, Chicago, Ill.) to remove any remaining dust. A laboratory-scale rice sizing device (Model 61-117-01, Grainman Machinery Manufacturing, Miami, Fla.) was used for separating broken kernels from head rice. Whole kernels were regarded as rice kernels with at least ¾ of the length of a milled whole kernel which is defined as head rice yield (HRY). Subsequent analysis was performed on the milled whole kernels.

3.3.4 Color Analysis

The color of the whole rice kernels was measured using an image analysis system (WinSEEDLE Pro, 2005a™, Regent Instruments Inc., Sainte-Foy, Quebec, Canada). Approximately 100 head rice kernels were spread in thin layer on the acrylic tray sample holder and placed on the scanning bed. The software reports the area of each color classification and then the percentage of discoloration was calculated as the colored area divided by total projected area. The software was calibrated with discolored kernels which were defined as follows: translucent white, opaque white, three shades of yellow, black/brown, red/brown, pink/red, and light pink.

3.3.5 Viscosity Analysis

30-g of milled rice were ground into flour with a cyclone mill (Udy Corporation, Ft. Collins, CO). Pasting properties of samples were measured with viscometer (RVA Super4, Newport Scientific,

Warriewood, Australia). Pasting viscosity profiles were determined by mixing 3 ± 0.01 g of flour with 25 ± 0.05 mL deionized water to form a slurry (AACC, 2000). The slurry was agitated at 150 rpm for 10 s for thorough dispersion. The Rapid Viscosity Analyzer (RVA) was set up on a 12.5 min runtime (50°C for 1.0 min, then heated at 95°C in 3.8 min, held at 95°C for 2.5 min, and then cooled to 50°C in 3.8 min and held at 50°C for 1.4 min). A thermogram was produced by the viscometer software showing viscosities in centipoise (cP).

3.3.6 Statistical Analysis

A three-way analysis of variance (ANOVA; JMP 14.0.0. SAS Institute, Cary, NC) was used to determine whether the three treatment factors including initial moisture content (IMC), storage temperature (T_s) and drying temperature (T_d) led to any significant changes in percentage point MC (PPMC) removal and milling characteristics (HRY, discoloration, pasting properties). A total of fifty-four rice samples were randomly assigned to treatment combinations (3 IMC levels × 3 T_s levels × 3 T_d levels × 2 replications). Significant differences between samples means were established using test at $\alpha = 0.05$.

3.4 Results and Discussion

3.4.1 Moisture Removal

Analysis of the impact of storage conditions and drying air temperature on the percentage point MC (PPMC) removal of rice samples is shown in Table 3.1. Drying air temperature and storage temperature had significant impact on the PPMC removal (p-value<0.05). About 89% of the variability in PPMC removal is explained by the statistical model. Root mean square error indicates only 0.11% of the mean of response is unaccounted for implying a good fit.

Table 3.1 Statistical significance test of the treatment factors including drying air temperature (Td), storage temperature (Ts), and their interactions in percentage point MC (PPMC) removal and milling characteristics (HRY, discoloration, pasting properties) as response variables of the experiment at $\alpha = 0.05$. n.s. indicates not significant; HRY indicates head rice yield.

Response variable	**P-value**			**Model Fit**
	T_d	T_s	$T_d \times T_s$	R^2
PPMC	<0.05	<0.05	n.s.	0.89
HRY	<0.05	n.s.	n.s.	0.86
Discoloration	n.s.	<0.05	n.s.	0.66
Peak viscosity	<0.05	<0.05	n.s.	0.82
Final viscosity	<0.05	<0.05	n.s.	0.77
Breakdown	<0.05	<0.05	n.s.	0.79
Setback	n.s.	<0.05	<0.05	0.69
Pasting temperature	<0.05	<0.05	<0.05	0.76

Table 3.2 shows moisture contents after each drying pass and PPMC removal for the hybrid long grain rice (XL745) with actual IMC of the rice sample stored at indicated storage temperatures (T_s = 10°C, 15°C, and 20°C). Rough rice exposed to relatively low temperature air (35°C) lost a relatively small amount of moisture (~2%-3%) after two-pass drying. However, drying air temperature of 60°C resulted in removal of 2.57-6.77 PPMC removal after two-passes drying. In this study, EMCs corresponding to the drying air conditions of 60°C, 45°C, and 35°C at 20% RH were 5.77%, 6.64%, and 7.33%, respectively. According to the finding by Cnossen et al. (2002), drying rate increased significantly with decreasing EMC; this therefore explained the reason behind significant reduction in MC for high-temperature drying air (60°C).

Table 3.2 Moisture contents after each drying pass and percentage point moisture content removal for hybrid long grain rice (XL745) with actual initial moisture content stored at indicated storage temperatures (Ts = 10°C, 15°C, and 20°C) and dried at drying air temperatures (Td = 35°C, 45°C, and 60°C). Mean and standard error (% ± SE) with the same type of letters are not significantly different at α = 0.05 using the Tukey's honest significant difference (HSD) test. IMC indicates initial moisture content; w.b. represents wet basis; MC represents moisture content; PPMC indicates percentage point MC removal.

IMC (%w.b.)	T_s (°C)	T_d (°C)	Actual IMC (%w.b.)	MC after 1st drying pass (%w.b.)	MC after 2nd drying pass (%w.b.)	PPMC (percentage points)
16	10	35	17.07	16.66	15.51	1.56±0.09 ^{f}
		45	17.24	16.68	15.22	2.03±0.3 ^{ef}
		60	16.63	16.06	13.68	2.95±0.24 ^{cdef}
	15	35	17.02	16.51	15.38	1.64±0.66 ^{ef}
		45	17.15	16.88	14.83	2.32±0.22 ^{cdef}
		60	16.75	15.94	13.19	3.57±0.02 ^{cdef}
	20	35	17.09	15.76	14.63	2.46±0.11 ^{def}
		45	17.12	15.72	13.93	3.19±0.8 ^{cde}
		60	16.60	14.24	12.53	4.07±0.42 ^{cd}
19	10	35	19.99	19.59	18.12	1.87±0.86 ^{cdef}
		45	19.59	19.02	16.98	2.61±0.17 ^{cdef}
		60	19.91	17.65	17.12	2.79±0.93 ^{cdef}
	15	35	19.97	19.83	17.5	2.48±0.82 ^{ef}
		45	19.43	18.54	16.93	2.50±0.6 ^{cdef}
		60	19.8	18.09	16.69	3.11±0.15 ^{cdef}
	20	35	20.13	19.47	18.13	2.0±0.69 ^{cdef}
		45	19.49	19.17	17.33	2.16±0.11 ^{ef}
		60	19.84	18.79	17.28	2.57±0.78 ^{cdef}
21	10	35	21.84	20.85	19.63	1.85±0.37 ^{ef}
		45	21.01	20.03	17.82	3.19±0.63 ^{cdef}
		60	21.23	20.89	17.92	3.31±0.24 ^{cdef}
	15	35	21.02	20.21	19.01	2.01±0.56 ^{def}
		45	21.35	19.4	17.94	3.41±0.22 ^{cdef}
		60	20.71	17.72	14.48	6.23±0.35 ^{ab}
	20	35	21.07	20.08	18.22	2.85±0.49 ^{cdef}
		45	20.83	18.3	16.63	4.19±0.46 ^{bc}
		60	20.89	17.79	14.11	6.77±0.21 ^{a}

The Arrhenius equation and activation energy may help describe the relationships observed between drying air temperature and moisture movement characteristics. Generally, as temperature increases, molecules gain energy and move faster. Therefore, the greater the drying air

temperature, the higher the energy level of the water molecules and thus the probability that more water molecules will evaporate during the drying process. Addition of thermal energy into the rice kernels initiates moisture migration. Lu and Siebenmorgen, (1992) reported that the diffusivity of moisture in rice kernel increased with increasing temperature according to Arrhenius-type function. Steffe and Singh (1980) used the Arrhenius-type function below to explain the diffusivity of moisture in rough rice components:

$$D = A\ exp\left(-\frac{B}{T_a}\right) \quad \text{Eq 3.2}$$

where D is the diffusivity of moisture (m^2/h), A and B are constants, and T_a is the absolute temperature (K). Steffe and Singh, (1980) reported that changes in the diffusivity of moisture in rice kernel could be attributed to grain type, drying conditions and grain geometry. Dong et al. (2009) also reported that at a high moisture gradient, the moisture diffused rapidly from the inside of the grain to its surface.

Rice samples with IMC=16% and IMC=21% stored at 10°C for all studied drying temperatures (35°C, 45°C and 60°C) had less MC removed than those stored at 15°C and 20°C. However, the same result was not observed for sample with IMC=19%. For example, PPMC removal for samples with IMC=21% stored at 10°C, 15°C and 20°C followed by drying at air temperature of 60°C was 3.31, 6.23 and 6.77, respectively.

3.4.2 Drying Rate Constant and Rice Material State Transitions

The thin layer drying equation of ASAE Standard S448 was used to calculate the drying rate constant k (ASAE Standards, 1999):

$$MR = \frac{MC-EMC}{IMC-EMC} = exp(-kt) \quad \text{Eq 3.3}$$

where MR is moisture ratio of the rice after a drying duration of t (min), MC is moisture content of the rice (decimal dry basis, d.b.), EMC is equilibrium moisture content (decimal d.b.) of the rice

corresponding to the drying air, IMC is initial moisture content (decimal d.b.), k is drying rate constant (min-1). Figure 3.1 shows the drying rate constant k versus three different drying air conditions (35°C, 20% RH; 45°C, 20% RH; 60°C, 20% RH) after 2nd drying pass. The drying rate constant is an important parameter that reflects the rate at which water is removed from the kernel (Cnossen et al., 2002). The drying rate increased when drying air temperature increased (Figure 3.1). Drying rate constant k for rice samples with IMC=16% and IMC=21% stored at 10°C for all studied drying temperatures (35°C, 45°C and 60°C) was less than those stored at 15°C and 20°C (Figure 3.1a and Figure 3.1c). However, drying rate constant k for samples with IMC=19% for all studied drying temperatures and storage conditions did not follow the same pattern (Figure 3.1b). Rice state transitions were assessed to help understand reasons for changes and trends of drying rate constant k in the different cases that were studied.

Figure 3.2 shows the state diagram of the rice kernel surface after 1st drying pass and 2nd drying pass for each drying air temperatures. When using a drying air temperature of 35°C, drying occurred primarily in the glassy region for most kernels and was, therefore, slower (low drying constant) than when drying above T_g in the rubbery region. In the glassy region, the overall drying process was slower compared to the rubbery region. However, there was no sharp state transitions for kernels with IMC=19%.

At a given MC, the temperature of the material relative to its T_g will determine whether the material will be in the glassy or the rubbery state. Researchers have used state diagrams and the concept of glass transition to predict changes in food properties and reaction kinetics below and above T_g (Peleg, 1996). As the kernel temperature increase above the T_g, the starch transforms to a rubbery state whereby its macromolecular structures have greater free volume, and thereby water in the starch is more mobile. Therefore, the rice kernel has a higher expansion coefficient, higher specific

volume, and higher heat and mass diffusivities (Cnossen et al., 2002). At the beginning of drying, the rice kernels were in the glassy state because their initial temperatures and moisture contents were about 10°C-20°C and 16%-21%, respectively. During drying, the temperature of the rice samples increased rapidly in the 1st drying pass. The starch in the kernel stored at 10°C was mostly in the glassy state during the 1st drying pass which means the moisture diffusion out of the rice kernel was slow. The glass transition temperatures in Figure 3.2 were calculated based on the equation which was developed for rice variety Drew (Siebenmorgen et al., 2004). Meesukchaosumran and Chitsomboon (2018) pointed out that there are upper and lower bounds at a 95% confidence level next to T_g line; these bounds or deviations may be due to differences in amylopectin percentage in starch composition of different rice cultivars. Therefore, at a given MC, samples stored at 20°C has less temperature gradient difference with T_g line, which means that most part of the kernel was in the rubbery, hence more PPMC removal during drying; the kernel would be expected to dry faster. In most of the runs, PPMC removal after 2nd drying pass was higher than PPMC removal after 1st drying pass. When the drying of rice sample is temporarily stopped after 1st drying pass and subjected to tempering (at T_d for 4 h), the moisture within the rice kernel diffuses to outer layer and surface. Therefore, there is more moisture available on the surface to evaporate as the rice undergo the 2nd drying pass.

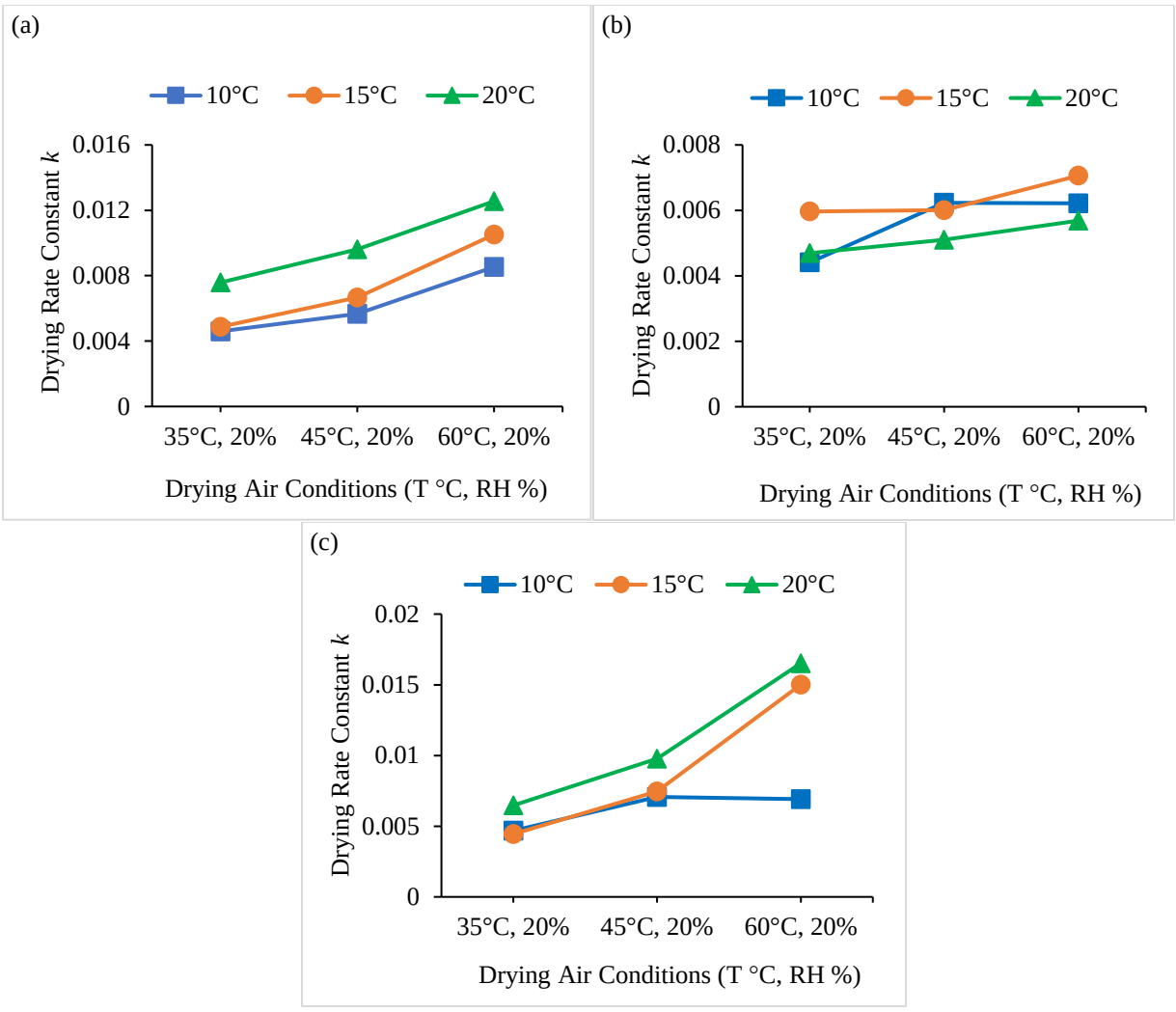

Figure 3.1 Drying rate constant k versus three different drying air conditions (T °C, RH %) after 2nd drying pass for hybrid long-grain XL745 rice at indicated storage temperatures (10°C, 15°C, and 20°C) (a) IMC=16% w.b., (b) IMC=19%w.b., (c) IMC=21% w.b.; T and RH indicate drying air temperature and relative humidity, respectively; IMC indicates initial moisture content; w.b. indicates wet basis.

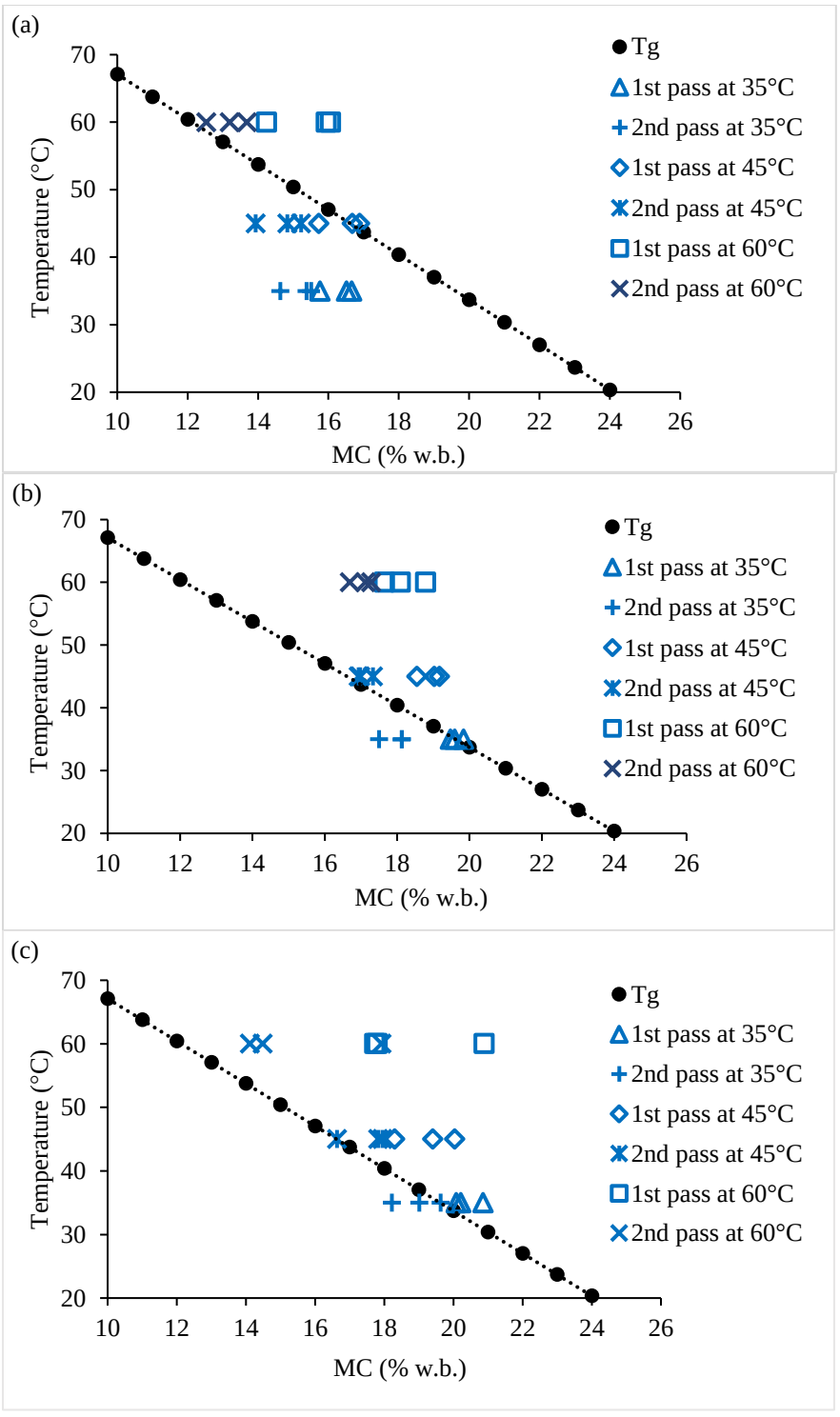

Figure 3.2 Kernel surface location after each drying pass at studied drying temperatures (35°C, 45°C, and 60°C) plotted onto a state diagram for hybrid long-grain XL745 rice (a) IMC=16% w.b., (b) IMC=19%w.b., (c) IMC=21% w.b.; IMC indicates initial moisture content; w.b. indicates wet basis.

3.4.3 Milling Charachteristics (Head Rice Yield and Discoloration)

Table 3.1 indicates the impact of storage conditions and drying air temperature on the HRY and discoloration of rice samples; Table 3.3 indicates mean values of HRY and discoloration after two-passes drying. Only drying air temperature had significant impact on the HRY (p-value<0.05). About 86% of the variability in HRY is explained by the statistical model. Root mean square error indicates only 0.14% of the mean of response is unaccounted for implying a good fit. The least square mean HRYs of samples dried with drying air of 35°C, 45°C, and 60°C in two passes and exposed to 4 h tempering, were 58.24%, 56.92%, and 53.89%, respectively. Loss of HRY was significant (p-value<0.05) for samples dried using high-temperature drying air (60°C). There was no significant difference in HRY between drying air temperatures of 35°C and 45°C. The lowest HRY (M=51.4%) corresponded to sample with IMC=21% stored at 10°C and dried using air at 60°C. Meanwhile, the highest HRY (M=58.8%) corresponded to sample with IMC=21% stored at 10°C and dried using air at 35°C. Ondier et al. (2012) suggested that maintaining the entire kernel in the rubbery state throughout high-temperature drying would prevent intra-kernel stress development and minimize fissuring. Using drying air of 60°C in samples with IMC=21% stored at 10°C which had less PPMC removal than those sample stored at 20°C, effected HRY (Table 3.1). The temperature gradients inside the kernel stored at 10°C and dried by heated air at 60°C is higher than those stored at 20°C. It is speculated that the temperature gradients inside the rice kernel contributed to fissuring. On the other hand, moisture gradients of the samples stored at 20°C was higher than those stored at 10°C (low drying rate). Based on this observation, the impact of moisture gradients on fissuring is minimal. The high temperature gradient might tend to mend fissures within the kernel, especially at a high IMC. Based on the PPMC removal and HRY results,

it can be concluded that high MC removal and milling yield could be achieved in samples stored at 10°C with initial MC of 16% followed by drying with air at 60°C.

Table 3.3 Mean values of head rice yield (HRY) and discoloration of hybrid long grain rice (XL745) with initial moisture content stored at indicated storage temperatures (Ts = 10°C, 15°C, and 20°C) and dried at drying air temperatures (Td = 35°C, 45°C, and 60°C). Mean and standard error (% ± SE) with the same type of letters are not significantly different at α = 0.05 using the Tukey's honest significant difference (HSD) test. IMC indicates initial moisture content; w.b. represents wet basis.

IMC (% w.b.)	T_s (°C)	T_d (°C)	HRY (%)	Discoloration (%)
16	10	35	57.6 ± 0.5 ^{abcd}	2.18 ± 0.89 ^{ab}
		45	55.9 ± 0.8 ^{abcde}	2.58 ± 0.6 ^{ab}
		60	55.15 ± 0.25 ^{abcde}	2.67 ± 0.16 ^{ab}
	15	35	56.75 ± 0.05 ^{abcd}	3.53 ± 0.35 ^{ab}
		45	55.75 ± 0.55 ^{abcde}	3.85 ± 1.17 ^{ab}
		60	52.01 ± 0.3 ^{de}	2.64 ± 0.33 ^{ab}
	20	35	57.55 ± 0.05 ^{ab}	3.49 ± 0.63 ^{ab}
		45	56.9 ± 0.5 ^{abcd}	3.10 ± 0.28 ^{ab}
		60	54.3 ± 1.9 ^{abcde}	3.34 ± 0.49 ^{ab}
19	10	35	56.75 ± 0.95 ^{abcd}	2.42 ± 1.38 ^{ab}
		45	56.7 ± 1.7 ^{abcd}	3.12 ± 0.31 ^{ab}
		60	51.25 ± 1.55 ^{e}	3.46 ± 0.16 ^{ab}
	15	35	55.7 ± 1.9 ^{abcde}	3.1 ± 0.74 ^{ab}
		45	55.1 ± 0.2 ^{abcde}	1.69 ± 0.3 ^{b}
		60	52.83 ± 0.77 ^{bcde}	5.09 ± 1.41 ^{ab}
	20	35	57.05 ± 0.25 ^{abc}	6.39 ± 1.28 ^{a}
		45	55.6 ± 0.05 ^{abcde}	3.97 ± 1.02 ^{ab}
		60	52.65 ± 0.95 ^{bcde}	5.79 ± 0.18 ^{ab}
21	10	35	58.8 ± 0.2 ^{a}	2.43 ± 0.39 ^{ab}
		45	55.95 ± 0.05 ^{abcde}	4.64 ± 0.44 ^{ab}
		60	51.4 ± 1.2 ^{e}	3.62 ± 0.49 ^{ab}
	15	35	57.15 ± 0.45 ^{abc}	3.85 ± 0.88 ^{ab}
		45	56.45 ± 0.05 ^{abcd}	3.32 ± 0.36 ^{ab}
		60	52.4 ± 0.2 ^{cde}	2.79 ± 0.83 ^{ab}
	20	35	57.2 ± 0.4 ^{abc}	4.01± 0.25 ^{ab}
		45	52.7 ± 0.1 ^{bcde}	3.86 ± 0.75 ^{ab}
		60	53.15 ± 0.75 ^{bcde}	5.14 ± 0.77 ^{ab}

Only storage temperature had significant impact on discoloration (p-value<0.05). About 66% of the variability in discoloration is explained by the statistical model. The least square mean (LS) discoloration of samples (XL745) stored at 20°C, 15°C, and 10°C were 4.40%, 3.32%, and 2.98%,

respectively. There was no significant difference in discoloration between storage temperatures of 15°C and 10°C (Table 3.2). All studied samples had discolored area less than 6% which is in good agreement with result reported by Shafiekhani et al. (2018). In those results, the authors reported that storage of rice even with high initial MC (21%) at 10°C, 15°C, and 20°C caused less than 10% discoloration after 16 weeks of storage (Shafiekhani et al., 2018).

3.4.4 Pasting Properties

Table 3.4 indicates pasting properties after two-passes drying of the hybrid long grain rice (XL745). Peak viscosity represents the maximum viscosity value reached during the heating phase. It is commonly used to indicate the extent of granules swelling during the gelatinization phase (Liang et al., 2003). In this study, storage temperature and drying air temperature had significant effect on peak viscosity (p-value<0.05). About 82% of the variability in peak viscosity is explained by the statistical model. Root mean square error indicates only 0.18% of the mean of response is unaccounted for, implying a good fit (Table 3.1). There was a significant difference on peak viscosities of samples stored at studied temperatures. The least square mean (LS) peak viscosity of samples (XL745) stored at 20°C, 15°C, and 10°C, were 2861.38cP, 2752.66cP and 2616.16cP, respectively. Peak viscosity increased with increasing drying air temperatures and were significantly greater ($p<0.05$) at 60°C.

Table 3.4 Mean values of pasting properties of hybrid long grain rice (XL745) with initial moisture content stored at indicated storage temperatures (Ts = 10°C, 15°C, and 20°C) and dried at drying air temperatures (Td = 35°C, 45°C, and 60°C). Mean and standard error (% ± SE) with the same type of letters are not significantly different at α = 0.05 using the Tukey's honest significant difference (HSD) test. IMC indicates initial moisture content; w.b. represents wet basis; cP indicates centipoise.

IMC (% w.b.)	T_s (°C)	T_d (°C)	Peak viscosity (cP)	Final viscosity (cP)	Breakdown (cP)	Setback (cP)	Pasting temp (°C)
16	10	35	2650 ± 45 ^{abc}	2931 ± 32 ^{abc}	1016 ± 12.3 ^{abc}	371 ± 0.5 ^{ab}	80.05 ± 0.03 ^{ab}
		45	2456.5 ± 52.5 ^{c}	2841.5 ± 7.5 ^{c}	966 ± 56 ^{c}	385 ± 45 ^{ab}	85.92 ± 0.42 ^{a}
		60	2713.5 ± 37.5 ^{abc}	3007 ± 23 ^{abc}	1143.5 ± 40.5 ^{abc}	293.5 ± 60.5 ^{ab}	80.35 ± 1.15 ^{ab}
	15	35	2742 ± 25 ^{abc}	3017 ± 40 ^{abc}	1167.5 ± 31.5 ^{abc}	275 ± 15 ^{ab}	79.22 ± 0.02 ^{b}
		45	2713 ± 36 ^{abc}	3007.5 ± 25.5 ^{abc}	1126.5 ± 17.5 ^{abc}	294.5 ± 10.5 ^{ab}	79.17 ± 0.02 ^{b}
		60	2789.5 ± 24.5 ^{abc}	3080.5 ± 9.5 ^{abc}	1165.5 ± 20.5 ^{abc}	291 ± 15 ^{ab}	79.62 ± 0.37 ^{b}
	20	35	2938.5 ± 3.5 ^{a}	3108 ± 57 ^{abc}	1313.5 ± 54.5 ^{a}	169.5 ± 60.5 ^{ab}	78.77 ± 1.17 ^{b}
		45	2802 ± 32 ^{abc}	3040.5 ± 26.5 ^{abc}	1213 ± 49 ^{abc}	238.5 ± 58.5 ^{ab}	78.82 ± 0.37 ^{b}
		60	2795 ± 14 ^{abc}	3084 ± 46 ^{abc}	1226.5 ± 60.5 ^{abc}	289 ± 60 ^{ab}	80.37 ± 2.35 ^{ab}
19	10	35	2677 ± 5 ^{abc}	3058 ± 4 ^{abc}	1045.5 ± 10.5 ^{abc}	381 ± 9 ^{ab}	78.77 ± 2.32 ^{b}
		45	2471 ± 55 ^{bc}	2884 ± 46 ^{bc}	966.5 ± 19.5 ^{c}	413 ± 9 ^{a}	83.15 ± 0.01 ^{ab}
		60	2831.5 ± 118.5 ^{abc}	3075 ± 6 ^{abc}	1231 ± 139 ^{abc}	243.5 ± 112.5 ^{ab}	81.52 ± 0.4 ^{ab}
	15	35	2807.5 ± 41.5 ^{abc}	3082.5 ± 31.5 ^{abc}	1178.5 ± 32.5 ^{abc}	275 ± 10 ^{ab}	78.45 ± 0.8 ^{b}
		45	2659.5 ± 24.5 ^{abc}	2980 ± 24 ^{abc}	1060.5 ± 22.5 ^{abc}	320.5 ± 0.5 ^{ab}	78.8 ± 0.02 ^{b}
		60	2790.5 ± 156.5 ^{abc}	3061.5 ± 66.5 ^{abc}	1177 ± 110 ^{abc}	271 ± 90 ^{ab}	80.8 ± 1.2 ^{ab}
	20	35	2876 ± 31 ^{a}	3091 ± 56 ^{abc}	1239.5 ± 26.5 ^{abc}	215 ± 25 ^{ab}	79.17 ± 0.01 ^{b}
		45	2701.5 ± 86.5 ^{abc}	2981.5 ± 0.5 ^{abc}	1155 ± 105 ^{abc}	280 ± 86 ^{ab}	80.45 ± 0.42 ^{ab}
		60	2942 ± 75 ^{a}	3192.5 ± 80.5 ^{a}	1300.5 ± 6.5 ^{ab}	250.5 ± 5.5 ^{ab}	80.85 ± 3.17 ^{ab}
21	10	35	2697 ± 11 ^{abc}	3012.5 ± 6.5 ^{abc}	1077.5 ± 23.5 ^{abc}	315.5 ± 17.5 ^{ab}	78.72 ± 0.42 ^{b}
		45	2465.5 ± 163.5 ^{bc}	2822.5 ± 136.5 ^{c}	1007 ± 56 ^{bc}	357 ± 27 ^{ab}	82.37 ± 3.17 ^{ab}
		60	2673.5 ± 107.5 ^{abc}	3001 ± 74 ^{abc}	1118 ± 17 ^{abc}	327.5 ± 33.5 ^{ab}	84.35 ± 0.45 ^{ab}
	15	35	2719 ± 49 ^{abc}	3038 ± 37 ^{abc}	1095 ± 17 ^{abc}	319 ± 12 ^{ab}	79.2 ± 0.05 ^{b}
		45	2637.5 ± 28.5 ^{abc}	2931.5 ± 37.5 ^{abc}	1091 ± 12 ^{abc}	294 ± 9 ^{ab}	79.97 ± 0.77 ^{ab}
		60	2915.5 ± 38.5 ^{a}	3096.5 ± 19.5 ^{abc}	1299 ± 6 ^{ab}	181 ± 19 ^{ab}	80.35 ± 0.45 ^{ab}
	20	35	3023 ± 48 ^{a}	3163 ± 64 ^{ab}	1322 ± 10 ^{a}	140 ± 16 ^{b}	79.12 ± 0.02 ^{b}
		45	2822.5 ± 32.5 ^{abc}	3035 ± 3 ^{abc}	1221 ± 55 ^{abc}	212.5 ± 29.5 ^{ab}	79.17 ± 0.02 ^{b}
		60	2852 ± 69 ^{ab}	3141.5 ± 68.5 ^{ab}	1177 ± 14 ^{abc}	289.5 ± 0.5 ^{ab}	81.55 ± 0.05 ^{ab}

Final viscosity represents the ability of the starch to form a viscous paste or gel after cooking and cooling. Drying air temperature and storage temperature had significant effect on final viscosity (p-value<0.05). About 77% of the variability in final viscosity is explained by the statistical model. The least square mean final viscosity of samples (XL745) stored at 20°C, 15°C, and 10°C, were 3093.0cP, 3032.77cP and 2959.16cP, respectively. Ambardekar and Siebenmorgen (2012) reported that peak and final viscosities increase with increasing drying air temperatures. Champagne et al. (1998) reported that the high peak and final viscosities of rice resulting at high drying temperature are associated with increased cooked rice cohesiveness.

Breakdown viscosity represents the starch granules disruption and it is commonly used as a measure of paste stability (Zaidul et al., 2007). The analysis of breakdown viscosity indicates that the granule rigidity was significantly affected by drying temperature and storage temperature. The lowest breakdown viscosity (M=966cP) was obtained in samples with IMC = 16% stored at 10°C with drying air temperature of 45°C (Table 3.4).

Setback viscosity reveals the gelling ability or the retrogradation tendency of starch during cooling phase (Zaidul et al., 2007). The results from this study have shown that storage temperature and interaction between storage temperature and drying air temperature affected setback viscosity. For setback viscosity, the samples stored at 10°C showed a higher setback viscosity (LS=343cP) than did the sample from the other storage temperatures of 15°C (LS=280.11cP) and 20°C (LS=231.61cP). The increase in setback viscosity (M=413cP) represents higher hardness of sample with IMC=19% stored at 10°C using drying air at 45°C (Table 3.4).

Pasting temperature represents the temperature at which the starch viscosity starts to rise during heating process (Liang et al., 2003). The statistical analysis of this study has shown that pasting temperature of rice is a function of drying air temperature, storage temperature and interaction

effect between drying air temperature and storage temperature. The highest pasting temperature (M=85.92°C) was found in samples with IMC=16% stored at 10°C with drying air temperature of 45°C (Table 3.4).

Generally, storage temperature and drying air temperature had significant affect (p-value<0.05) on functional properties of the samples in this study. Dillahunty et al. (2001) reported that viscosity was affected by exposure duration and temperature. Higher PPMC removal for samples dried with air at 60°C indicate the reduced water absorption of samples (Table 3.2). The reduction of water content and absorption at higher grain temperature can result in and be attributed to the rearrangement of starch granules after drying, respectively (Inprasit and Noomhorm, 2001). Borompichaichartkul et al. (2007) and Ondier et al. (2013) pointed out that higher final and peak viscosities are the indications of higher values of kernel hardness, which is highly correlated with better cooking quality. Thus, temperature of drying air and rate of water removal affected physicochemical properties of milled rice.

3.5 Conclusion

This study documented the moisture removal, material state transition, milling and quality characteristics of hybrid long grain rice (XL745) subjected to chilling followed by drying with slightly heated and high temperature air drying methods. Drying air temperature of 60°C resulted in PPMC removal of 2.57-6.77 after two-passes drying. Samples with IMC=16% and IMC=21% stored at 20°C had higher drying rate constant than those stored at 10°C. High drying air temperature (60°C) caused reduction in HRY (HRY=51.4% versus those at 45°C and 35°C, HRY=55.95% and HRY=58.8%, respectively) for samples with IMC=21% and stored at 10°C pre-drying. Chilling/cold storage of high MC rough rice at 10°C, 15°C, 20°C retarded discoloration of milled rice. Viscosity of milled rice sample was affected by drying air temperature and pre-drying

storage temperature. In accordance with our hypothesis, this research showed that the rough rice drying behavior and quality of milled rice are tied to pre-drying chilling procedure and subsequent drying conditions. The findings from this study provide useful information for rice growers and processors on impacts of the chilling aeration technology on rice moisture removal, material state transition, milling and quality characteristics. Based on limited information of the heat and mass transfer of rough rice subjected to chilled environment, the following research is suggested for future work: 1) develop the prediction equation to determine EMC values of rough rice at chilled environment, 2) evaluate the drying energy efficiency and overall drying cost associated with the new methods of post-harvest rice management using cold storage and chilling aeration.

Acknowledgment

The authors acknowledge the University of Arkansas Division of Agriculture, and the Rice and Grain Processing program for collaboration and providing facilities. The authors also acknowledge FrigorTec Americas Inc., especially through Johannes Karcher for support and cooperation during the research. The authors also wish to acknowledge Dr. Rusty Buatista of RiceTech for help with scrutiny of data. This study was based upon work that is supported, in part, by the United States Department of Agriculture National Institute of Food and Agriculture Hatch Act Funding.

3.6 References

AACC, Approved Method of the AACC. (2000). Method 61-02 for RVA, ninth ed. American Association of Cereal Chemists, St. Paul, MN.

Ambardekar, A. A., and Siebenmorgen, T. J. (2012). Effects of postharvest elevated-temperature exposure on rice quality and functionality. *Cereal. Chem.*, 89(2), 109-116.

Amiri, A., Mousakhani-Ganjeh, A., Shafiekhani, S., Mandal, R., Singh, A. P., Esmaeilzadeh Kenari, R. (2019). Effect of high voltage electrostatic field thawing on the functional and physicochemical properties of myofibrillar proteins. *Innov. Food Sci. Emerg. Technol.*, 56, 102191.

Anari, A., Mai, C., Sengupta, A., Howard, L., Brownmiller, C., Wickramasinghe, S. R. Combined

Osmotic and Membrane Distillation for Concentration of Anthocyanin from Muscadine Pomace. *J. Food. Sci.*, 84(8), 2199-2208.

ASABE Standards, 45th Ed. (1998). Moisture relationship of plant based agricultural products. St. Joseph, Mich.: ASAE.

ASAE Standards, 46th Ed. (1999). S448. Thin layer drying of grains and crops. St. Joseph, Mich.: ASAE.

ASABE Standards. (2008). S352.2 APR1988 (R2008): Moisture measurement - Unground grains and seeds. St. Joseph, Mich.: ASABE.

Atungulu, G. G., and Shafiekhani, S. (2019). Reference on Rice Quality and Safety. In P. Gaspar, & P. da Silva (Eds.), Novel Technologies and Systems for Food Preservation (pp. 226-274). Hershey, PA: IGI Global.

Borompichaichartkul, C., Wiset, L., Tulayatun, V., Tuntratean, S., Thetsupamorn, T., Impaprasert, R., Waedalor, I. (2007). Comparative study of effects of drying methods and storage conditions on aroma and quality attributes of Thai jasmine rice. *Dry. Technol.*, 25(7), 1185-1192.

Brunner, H. (1989). Grain preservation by means of refrigeration in tropical countries. Sulzer Technical Review 411989. Winterthur, Switzerland: Sulzer Brothers.

Champagne, E. T., Lyon, B. G., Min, B. K., Vinyard, B. T., Bett, K. L., Barton, F. E., II, Webb, B. D., McClung, A. M., Moldenhauer, K. A., Linscombe, S., McKenzie, K. S., and Kohlwey, D. E. (1998). Effects of postharvest processing on texture profile analysis of cooked rice. *Cereal Chem.*, 75, 181-186.

Chek, T. I. (1989). Application of paddy cooling technique in Malaysian rice industry. Workshop on Grain Drying, Bulk Handling, Storage Systems in ASEAN. Pitsanuloke, Thailand.

Cnossen, A. G., Siebenmorgen, T. J., Yang, W. (2002). The glass transition temperature concept in rice drying and tempering: effect on drying rate. *Trans. ASABE.*, 45(3), 759-766.

Cooper, N. T. W., Siebenmorgen, T. J. (2007). Correcting head rice yield for surface lipid content (degree of milling) variation. *Cereal. Chem.*, 84(1), 88-91.

Dillahunty, A. L., Siebenmorgen, T. J., Buescher, R. W., Smith, D. E., Mauromoustakos, A. (2001). Effect of temperature, exposure duration, and moisture content on color and viscosity of rice. *Cereal. Chem*., 78(5), 559-563.

Dong, R., Lu, Z., Liu, Z., Nishiyama, Y., Cao, W. (2009). Moisture distribution in a rice kernel during tempering drying. *J. Food. Eng*., 91(1), 126-132.

Inprasit, C., Noomhorm, A. (2001). Effect of drying air temperature and grain temperature of different types of dryer operation on rice quality. *Dry. Technol*., 19(1), 389-404.

Liang, X., King, J. M. (2003). Pasting and crystalline property differences of commercial and isolated rice starch with added amino acids. *J. Food. Sci*., 68(3), 832-838.

Lu, R., Siebenmorgen, T. J. (1992). Moisture diffusivity of long-grain rice components. *Trans. ASAE*., 35(6), 1955-1961.

Luthra, K., Shafiekhani, S., Stephens, B., Sadaka, S., Atungulu, G. G. (2019). Evaluation of the performance of a newly developed wireless temperature and moisture sensor for rice under various levels of temperature, moisture content and dockage. *Trans. ASABE*., 35(3), 311-318.

Maier, D. E., Bakker-Arkema, F. W., Moreira, R. G. (1992). Comparison of conventional and chilled aeration of grains under Texas conditions. *Appl. Eng. Agric*., 8(5), 661-667.

Meesukchaosumran, S., Chitsomboon, T. (2018). Effects of resting periods, air temperatures, and air velocities on free-fall paddy dryer performances. *Suranaree. J. Sci. Technol*., 25(1), 11-26.

Navarro, S., Noyes, R., Armitage, D., Maier, D. (2002). Objectives of aeration. In: The Mechanics and Physics of Modern Grain Aeration Management, 1-34, ed. S. Navarro and R. Noyes. Boca Raton: CRC Press.

Ondier, G. O., Siebenmorgen, T. J., Mauromoustakos, A. (2012). Drying characteristics and milling quality of rough rice dried in a single pass incorporation glass transition principle. *Dry. Technol*., 30(16), 1821-1830.

Ondier, G. O., Siebenmorgen, T. J., Mauromoustakos, A. (2013). Physicochemical properties of rice dried in a single pass using high temperatures. *Cereal Chem.*, 90(5), 502-506.

Peleg, M. (1996). On modeling changes in food and bio-solids at and around their glass transition temperature range. CRC Critical Reviews in Food Science and Nutrition, 36(1), 49-67.

Rius, J. (1987). Experiences with storage of paddy using Granifrigors. Messr. Conserga, Spain.

Schluterman, G. J., Siebenmorgen, T. J. (2004). Air and rice property profiles within a commercial cross-flow rice dryer. *Appl. Eng. Agric*., 20(4), 487-494.

Siebenmorgen, T. J., Yang, W., Sun, Z. (2004). Glass transition temperature of rice kernels determined by dynamic mechanical thermal analysis. *Trans. ASAE*., 47(3), 835-839.

Shafiekhani, S., Zamindar, N., Hojatoleslami, M., Toghraie, D. (2016). Numerical simulation of transient temperature profiles for canned apple puree in semirigid aluminum-based packaging during pasteurization. *J. Food Sci. Technol.* 53(6), 2770-2778.

Shafiekhani, S., Atungulu, G. G. (2017). Kinetics of mold growth and rice quality metrics during storage as affected by pre-harvest fungicide application. ASABE Annual International Meeting, doi: 10.13031/aim.201700818.

Shafiekhani, S., Wilson, S. A., Atungulu, G. G. (2018). Impacts of storage temperature and rice

moisture content on color characteristics of rice from fields with different disease management practices. *J. Stored. Prod. Res*., 78, 89-97.

Shafiekhani, S., Lee, J. A., Atungulu, G. G. (2019). Prediction of rice milling and quality attributes during storage using regression analyses. *Trans. ASABE*., 62(5), 1259-1268.

Sharma, A. D., Kunze, O. R. (1982). Post-drying fissure developments in rough rice. *Trans. ASAE*., 25(2), 465-468, 474.

Steffe, J. F., Singh, R. P., Bakshi. A. S. (1979). Influence of tempering time and cooling on rice milling yields and moisture removal. *Trans. ASAE*., 22(5), 1214-1218, 1224.

Steffe, J. F., Singh, R. P. (1980). Liquid diffusivity of rough rice components. *Trans. ASAE*., 23(3), 767-774, 782.

Thorpe, G. R., Elder, W. B. (1982). Modelling the effects of aeration on the persistence of chemical pesticides applied to stored bulk grain. *J. Stored. Prod. Res*., 18, 103-104.

Yang, W., Jia, C. (2004). Glass transition mapping inside a rice kernel. *Trans. ASABE*., 47(6), 2009-2015.

Zaidul, I. S. M., Yamauchi, H., Kim, S. J., Hashimoto, N., Noda, T. (2007). RVA study of mixtures of wheat flour and potato starches with different phosphorus contents. *Food. Chem*., 102, 1105-1111.

Chapter 4: **Modeling heat and mass transfer of long-grain hybrid rice in a chilled environment**

4.1 Abstract

While chilling aeration technology for grains has found use in other countries, application for use in the USA for rice has been hampered due to lack of scientific and industry relevant data. The aim of this study is to determine the drying kinetics of rough rice at chilled environment; such data is vital for automated grain condition monitoring and control of aeration systems at chilled rice conditions. Adsorption and desorption isotherms of hybrid long-grain rough rice (XL-745) subjected to temperature environments that are typical in field chilled storage conditions (5 and 15°C) were measured. The dynamic vapor sorption analyzer (IGAsorp) consisting of microbalances in controlled atmosphere were used to generate predictive isotherms. Changes in sample weight were continuously monitored across a range of equilibrium relative humidity (10-70%) until a steady-state mass was attained. Nonlinear regression analysis was used to estimate empirical constants of five models used for describing grain sorption isotherms. The appropriateness of each model in describing the equilibrium data was evaluated to minimize the root mean square error (RMSE). The modified Chung-Pfost equation best described the experimental data with RMSEs of 0.557 and 0.912 for adsorption and desorption data, respectively. The equilibrium moisture content (EMC) of rice experimentally measured at the lowest extreme condition of 5°C with 10% relative humidity (RH) was 12.5% (dry basis). However, the EMC estimated using conventional modified Chung-Pfost equation was 8.9% (dry basis) which indicated a significant deviation in EMC value prediction with equations extrapolating data for chilling environments. All five prediction models (modified Chung-Pfost, modified Henderson, modified Oswin, modified Halsey, and modified GAB) were in good agreement for experimental

data at high temperature conditions (e.g. at 30°C). The results indicated that it is more accurate to use newly developed constants for EMC models of rice in chilled environment. The three-dimensional ellipsoid shape was used to describe the rough rice geometry. Mathematical models were developed to predict the moisture and temperature distribution during the drying processes at chilled conditions of 5°C and 15°C. The models were solved by finite element method using Comsol Multiphysics® simulation program. Increasing the drying temperature from 5°C to 15°C increased the effective moisture diffusivity from 9.0×10^{-13} to 1.1×10^{-12} m^2/s. The drying activation energy value reached 25.1 kJ/mol under chilled environment.

Keywords: Rough rice, Mathematical modeling, Equilibrium moisture content, Moisture diffusivity, Activation energy, Chilled environment.

4.2 Introduction

Chilling aeration of high-moisture rough rice may permit short- to long-term storage management of the grain entirely independent of ambient temperature and relative humidity conditions; this would reduce the throughput constraints on commercial and on-farm dryers to dry all fresh rice within two weeks following harvest. The use of mathematical models to describe the chilling aeration processes is very useful and allows the design and optimization of the equipment involved in the process (Iguaz et al., 2003). Thus, there is need to investigate how changes in temperature and relative humidity (RH) influence equilibrium moisture content (EMC) of rice under chilling environment.

EMC of rice is defined as the moisture content (MC) at which the rice kernels are neither gaining nor losing moisture. The EMC of rice depends on the temperature and RH of the surrounding air (Goneli et al., 2007; Ondier et al., 2012).

Transport phenomena which happens at the boundary surface of the grain and surrounding atmosphere involves adsorption and desorption. The rate at which adsorption and desorption happens depends on grain physical characteristics, such as roughness, porosity and chemical characteristics, e.g., hydrogen bonding and capillary forces (Wellingford and Labuza, 1983; Chen et al., 1984).

Different methods can be used to find the EMC isotherms for rough rice, but the most basic method is the static method (Iguaz and Versade, 2007). This method uses saturated salt solution wherein a sample is stored in an enclosure (e.g., desiccators) and is allowed to reach equilibrium with the surrounding atmosphere of known RH maintained by the salt solutions. The sample weight is measured at regular intervals until a constant weight is reached; at this point the moisture content is taken to be the EMC. This method requires long equilibration time, which is usually from 7 – 14 weeks for rough rice samples at temperatures of 4 – 40 ºC and RHs of 10 – 90% (Choi et al., 2010). Thus, it is questionable whether the microbial and physico-chemical stability remain valid in the sample during long experimental period, especially at higher water activity (Rahman and Sablani, 2009). The other method to create the EMC isotherm is by using dynamic vapor sorption (DVS). The DVS overcomes many of the disadvantages encountered with the static method. The DVS system does not require the use of saturated salt solutions in order to provide the desired RH, but instead, uses a mixture of dry nitrogen and saturated water vapor, whose proportions are precisely controlled by mass flow controller. The moisture balance is designed to measure weight loss changes over time until the rate of weight loss reaches a constant mode. Schmidt and Lee (2012) and Bingol et al. (2012) reported the comparison of water vapor sorption isotherms obtained using the dynamic method and those obtained using the static method. They pointed out that the

DVS differed dramatically from the saturated salt solution isotherms in water activity range of 0.4 – 0.8.

Many studies have employed the use of thin layer drying equations to determine the drying characteristics of grain exposed to controlled air conditions (Basunia and Abe, 2001; Prakash et al., 2017). In thin layer drying, all rice kernels are exposed to identical drying air conditions (Prakash and Siebenmorgen, 2018). ASABE Standard S448.2 (ASABE Standards, 2014) defined three layers of kernels as maximum layer depth for thin layer drying. Mathematical equations utilized for describing isotherms of hybrid long-grain rice are shown in Table 4.3. For the equations listed in Table 4.3, T is temperature (ºC), M_e is equilibrium moisture content (% dry basis), RH is relative humidity (decimal), and A, B and C are grain specific empirical constants. The mathematical equations have been successfully used by many authors to model sorption isotherms of rough rice (Iguaz and Virseda, 2006; Ondier et al., 2011). Studies have found that the parameters of thin layer drying equations depend upon the rice properties, such as harvest MC, chemical composition, and dimensions, as well as drying air properties, such as temperature, RH, and air velocity (Cnossen et al., 2002; Prakash et al., 2011). Considering that chilling aeration utilizes drying air temperatures that are not commonly used in the U.S. drying industry, there is need to evaluate the mathematical equations for estimating EMC and moisture movement at chilled environment conditions.

Drying involves simultaneous heat and mass transfer phenomena (Brooker et a., 1992). To design the effective drying equipment, it is necessary to understand the thermodynamic properties of moist air and rice drying kinetics. The effective moisture diffusivity (D_{eff}) and the activation energy (E_a) are important to study absorbed and desorbed water's properties and calculate the energy required in the drying process. Several studies have used single-kernel mathematical models to

describe the moisture movement within a single rice kernel and estimate moisture gradients and fissuring in rice (Yang et al., 2002; Meeso et al., 2007; Prakash and Pan, 2012). Developing the analytical solutions is complicated due to the irregular shape of rice kernel. Therefore, in this study numerical methods such as finite difference or finite element methods were used to solve the heat and mass transport equations in single kernel of rice following the work of Igathinathane et al. (1999) and Prakash et al. (2011). In this study, the three-dimensional heat and mass transport model was solved using Comsol Multiphysics® simulation program.

The objectives of this study were to: (1) measure the adsorption and desorption isotherms of long-grain rough rice subjected to chilled environment using DVS method; (2) determine parameters of the thin layer drying equations for each air condition; (3) evaluate the appropriateness of the equations for estimating equilibrium data of rough rice for the range of temperature and RH studied; (4) determine the moisture diffusivity and activation energy values associated with moisture and heat transport in chilled environment, and (5) perform mathematical modeling using finite element method to investigate the heat and mass transfer during drying at low temperatures.

4.3 Materials and Methods

4.3.1 Rice Sample

A hybrid long-grain rice cultivar XL-745 was harvested from Arkansas in the fall of 2018. Samples were cleaned with a dockage tester (model XT4, Carter-Day, Minneapolis, Minn.). Prior to equilibrium moisture content (EMC) experiments, three hundred kernels, 100 kernels for each replicate, were randomly selected and the moisture content (MC) of the subsample measured using single kernel moisture meter (Shizuoka Seiki CTR 800A). Bulk sample MCs were obtained by averaging 100 individual kernel MC. The rice samples were then double bagged in “Zip-loc” ® plastic bags and refrigerated at approximately 4ºC until testing.

4.3.2 Test System

Dynamic vapor sorption analyzer (IGAsorp, Hiden Isochema Ltd., Warrington, UK) was used to obtain EMC of rough rice. The IGAsorp is an ultrasensitive electro-balance with 0.05 µg resolution and a 1 g weighing capacity. Relative humidity (RH) is controlled within the IGAsorp by measuring a combination of dry and wet nitrogen (N_2) streams. Dry N_2 enters the instrument and is divided into two streams. The flow rate of each stream is controlled using a mass flow controller (MFC). One of the N_2 streams passes through a solvent reservoir, where it is saturated with the solvent at a set temperature. The dry N_2 is then combined with the wet N_2, and mixed stream flows into the sample chamber. A RH sensor with a measurement accuracy of ± 1% to 90% RH and ± 2% RH from 90% to 95% RH and a platinum resistance temperature detector (RTD) temperature probe (± 0.1 K) located inside the sample chamber provide proportional integral differential feedback control to the MFCs. The sample chamber and the solvent reservoir are controlled at same temperature using a temperature-controlled water bath (Minnick et al., 2018).

The isothermal kinetics of hybrid long-grain rice cultivar XL-745 were studied at chilling temperature levels of 5 and 15ºC; another run was conducted at 30ºC for the purpose of model comparisons and validations. For each studied temperature, three rice kernels were placed into the pan of the equipment. The RH was changed from 10% to 70% and, then back to 10% to capture adsorption and desorption isotherms of sample. The HIsorp software program intelligently controls the IGAsorp reservoir temperature to achieve the target flow rate (250 mL/min N_2) and RH conditions. Before running the isotherm tests, all the samples were gently conditioned by the IGAsorp which was programmed at 26ºC and 56% RH to attain the same starting EMC.

4.3.3 Effective Moisture Diffusivity and Activation Energy

Fick's diffusion equation as a governing equation of mass transfer is normally used to evaluate the diffusion of moisture from rice kernels during drying process (Khanali et al., 2016). Moisture diffusion of rice kernels during drying is a complex process which involves molecular diffusion, capillary flow, Knudsen flow, and surface diffusion. To account for both liquid and vapor phase diffusivity in rice kernel, usually an effective moisture diffusivity (D_{eff}) is used (Aguerre et al., 1982). The analytical solution of the diffusion equation based on Fick's second law with constant diffusion coefficient for spherical geometry is described by Crank as follows (Crank, 1975):

$$MR = \frac{M-M_e}{M_0-M_e} = \frac{6}{\pi^2}\sum_{n=1}^{\infty}\frac{1}{n^2}\exp\left(-\frac{n^2\pi^2 D_{eff}t}{r^2}\right) \quad \text{Eq 4.1}$$

Where *MR* is the moisture ratio (dimensionless), *M* is moisture content (%, d.b.) of the kernel at any given time *t*, M_e is the equilibrium moisture content (%, d.b.), M_0 is the initial moisture content (%, d.b.), *n* is the number of data points, D_{eff} is effective moisture diffusivity (m^2/s), and *r* is the equivalent radius of the rice kernel (m). Equivalent radius is determined by equating the volume of rice kernel (*V*, m^3) to that of sphere and is given by:

$$r = \left(\frac{3}{4\pi}V\right)^{0.33} \quad \text{Eq 4.2}$$

The volume (*V*) of rice kernel was determined using equation described by Mohsenin, 1986:

$$V = 0.25\left[\left(\frac{\pi}{6}\right)L(W+T)^2\right] \quad \text{Eq 4.3}$$

Where *L* (m) is length, *W* (m) is width, and *T* (m) is thickness of rice kernel.

Eq 4.1 could be further simplified into straight-line equation as shown in Eq 4.4 (Dadali et al., 2007):

$$\ln MR = \ln\left(\frac{6}{\pi^2}\right) - \left(\frac{\pi^2 D_{eff}}{r^2}\ t\right) \quad \text{Eq 4.4}$$

A straight line is obtained from Eq 4.4 by plotting *Ln (MR)* versus drying duration, and the D_{eff} for each temperature can be calculated from the slope:

$$Slope = \frac{\pi^2 D_{eff}}{r^2}$$ Eq 4.5

The temperature dependence of D_{eff} is usually expressed by an Arrhenius relationship as in Eq 4.6 (Cai and Chen, 2008):

$$D_{eff} = D_0 exp\left(-\frac{E_a}{R(T+273.15)}\right)$$ Eq 4.6

Where D_0 is the pre-exponential factor (m^2/s), E_a is the activation energy (kJ/mol), T is the drying temperature (ºC), and R is the universal gas constant (8.3143, kJ/mol K).

Taking natural logarithm of both sides of Eq 4.6, the result was given as follows:

$$\ln D_{eff} = \ln(D_0) + \frac{E_a}{R}\left(\frac{1}{T+273.15}\right)$$ Eq 4.7

The activation energy could be determined from the slope of the straight line formed by plotting *Ln* (D_{eff}) versus [1/(T+273.15)] such that the slope is E_a/R.

To determine the value of mass diffusion coefficient (D) according to the air temperature, the Arrhenius equation was used where the parameters a_1 = 0.0003 m^2/h and b_1 = -3023 K were obtained by fitting Eq 4.8 to the experimental data.

$$D = a_1 exp\left(\frac{b_1}{T_{abs}}\right)$$ Eq 4.8

4.3.4 Transport Equations

The following assumptions were made for these simulations:

- Liquid diffusion was considered as the mechanism of moisture movement within the rice kernel (Steffe and Singh, 1980);
- Rough rice kernel assumed to be an ellipsoid shape in the model (Prakash and Pan, 2012; Pereira et al., 2015);
- Shrinkage in size of the rice kernel during the drying simulation was neglected (Prakash and Pan, 2012);

- The presence of multiple components such as endosperm, bran and husk were not considered in model (Ece and Cihan, 1993).

Fick's second law of diffusion and Fourier's law of conduction in a three-dimensional Cartesian coordinate system (x, y, z) were used to model the moisture transport process and heat transfer within the rice kernel, respectively. Using symmetry about axes in an ellipsoid shaped model was solved in three-dimensional objects. The governing moisture and conduction transport equations with initial and boundary conditions are described below.

Governing moisture transport equation:

$$\frac{\partial M\,(x,y,z,t)}{\partial t} = D\nabla^2 M(x,y,z,t) \qquad \text{Eq 4.9}$$

Initial condition:

$$M(x,y,z,0) = M_i \qquad \text{Eq 4.10}$$

Boundary conditions:

The model was tested by comparing two different boundary conditions for moisture transport of rice kernel. Dirichlet boundary condition assumed the kernel surface moisture *M* (kg water/kg dry matter) to have the same moisture as the equilibrium moisture content M_e (kg water/kg dry matter) of rice in the ambient environmental conditions (Meeso et al., 2007):

$$M(x,y,z,t) = M_e \qquad \text{Eq 4.11}$$

Meanwhile, Newmann boundary condition equated the outward moving moisture flux to moisture taken away by convective air and obtained by following equation (Yang et al., 2002):

$$-D\nabla M(x,y,z,t) = h_m(M(x,y,z,t) - M_e) \qquad \text{Eq 4.12}$$

Where *t* is time (s), ∇ is divergence operator, *D* is moisture diffusivity (m^2/s), *M* is the moisture content (kg water/kg dry solids), M_i is the initial moisture content (kg water/kg dry solids), M_e is

the equilibrium moisture content of rice corresponding to ambient humidity conditions (kg water/kg dry solids), and h_m (m/s) is the surface mass transfer coefficient (m/s).

Governing heat transfer equation:

$$\rho c_p \frac{\partial T(x,y,z,t)}{\partial t} = k\nabla^2 T(x,y,z,t) + Q \quad \text{Eq 4.13}$$

Initial condition:

$$T(x,y,z,0) = T_i \quad \text{Eq 4.14}$$

Boundary condition:

The heat transfer by convective air to the rice surface can be equated to the conductive heat entering the surface and change in enthalpy of evaporating moisture. The heat transfer boundary condition can be described by following equation:

$$-k\frac{\partial T(x,y,z,t)}{\partial t} = h_c(T(x,y,z,t) - T_a) - \lambda h_m(M(x,y,z,t) - M_e) \quad \text{Eq 4.15}$$

Where ρ is density of rice (kg/m^3), C_p is specific heat (J.kg^{-1}.ºC^{-1}), T is temperature (ºC), k is thermal conductivity (W.m^{-1}.ºC^{-1}), ∇ is divergence operator, Q is volumetric heat generation (W/m^3), T_i (ºC) is the initial temperature of rice kernel, h_c (Wm^{-2} ºC^{-1}) is the convective heat transfer coefficient, T_a (ºC) is the temperature of drying air, λ (J/kg) is heat latent of vaporization, h_m (m/s) is the surface moisture transfer coefficient, M (kg water/kg dry matter) is kernel surface moisture, and M_e (kg water/kg dry matter) is the equilibrium moisture content of rice. The equilibrium moisture content of the rough rice (M_e) as a function of air temperature, T (ºC), and relative humidity, RH (decimal), was used in simulation of rough rice drying.

Surface mass transfer coefficient, h_m (m/s) and surface heat transfer coefficient, h_c (W.m^{-2}.K^{-1}) were determined using the following relationship (Fortes et al., 1981):

$$h_m = \frac{D_{AB}}{\mathrm{R}T_{abs}d_p}[2.0 + 0.6Re^{0.5}Sc^{0.33}] \quad \text{Eq 4.16}$$

$$h_c = \frac{k}{d_p}(2.0 + 0.6Re^{0.5}Pr^{0.33}) \quad \text{Eq 4.17}$$

Where D_{AB} is the vapor diffusivity in the air, h_m is the surface moisture transfer coefficient, h_c is the heat transfer coefficient, d_p is the particle equivalent diameter, R=287.035 J/kgK is universal constant for air, T_{abs} (K) is drying air temperature, Re is the Reynolds number, Pr is the Prandtl number, and Sc is the Schmidt number is obtained by the following expressions:

$$d_p = \left(L\frac{(W+T)^2}{4}\right)^{0.33} \quad \text{Eq 4.18}$$

$$B = \sqrt{WT} \quad \text{Eq 4.19}$$

$$A = \frac{\pi BL^2}{(2L-B)} \quad \text{Eq 4.20}$$

$$Re = \frac{\rho v D}{\mu} \quad \text{Eq 4.21}$$

$$Pr = \frac{c_p \mu}{k} \quad \text{Eq 4.22}$$

$$Sc = \frac{\mu}{\rho D_{AB}} \quad \text{Eq 4.23}$$

Where L is the length of major axis, W is width of intermediate axis, T is thickness of minor axis of rough rice kernel, A is surface area, ρ is air density (kg/m^3), v is air velocity (m/s), D is equivalent particle diameter of rice, μ is air viscosity (kg/ms), C_p is air heat capacity (J/kgK), k is air thermal conductivity (W/mK). Moisture gradient (MG) within the rough rice kernel model was determined in the simulation program using the following expression (Prakash and Pan, 2012):

$$MG = |\nabla M| = \left[\left(\frac{\partial M}{\partial x}\right)^2 + \left(\frac{\partial M}{\partial y}\right)^2 + \left(\frac{\partial M}{\partial z}\right)^2\right]^{1/2} \quad \text{Eq 4.24}$$

Where x (mm), y (mm), and z (mm) are the three coordinates.

4.3.5 Single Kernel Modeling

Several studies have reported on mathematical models for irregular shapes like rice kernel. Most of the times rice kernels are approximated to simpler shapes such as sphere, cylinder, prolate spheroid and ellipsoid (Steffe and Singh, 1980; Lu and Siebenmorgen, 1992; Igathinathane and

Chattopadhyay, 1999; Wu et al., 2004). Studies have shown that an ellipsoidal model (three-dimensional) may best resemble the kernel geometry and is appropriate for simulating the drying and adsorption process (Prakash et al., 2011; Pereira et al., 2015; Zhao et al., 2019).

Three dimensional models developed in this study were solved using Comsol Multiphysics® simulation program (Comsol Inc, Palo Alto), which uses the finite element method to solve the model equations. The average of the rice kernel size was used for generation of the geometry. The rough rice size was determined by Hacihafizoglu et al. (2008) where the authors calculate the averages for grain dimensions after taking measurement of 100 grains. Length, width, and thickness of rice kernel was measured and reported (Table 4.1). Mean values of the measured sizes were used to describe ellipsoidal geometry of rough rice kernels in the model. The measured values of volume V = 24.7 mm^3, the equivalent particle diameter d_p = 3.5 mm, the surface area A = 3.76 × 10^{-5} m^2. The unstructured tetrahedral mesh was generated with maximum and minimum element sizes of 0.387 mm and 0.00387 mm, respectively. The representative meshed model geometry of rough rice is shown in Figure 4.1. The number of elements in rough rice model of ellipsoid shape was 67186.

Table 4.1 Kernel dimensions of hybrid long-grain rice (XL-745) at 17.6% MC on w.b.

Hybrid LG (XL745)	**Length (mm)**	**Width (mm)**	**Thickness (mm)**
Mean	9.7	2.4	1.9
(Std.)	0.5	0.1	0.09

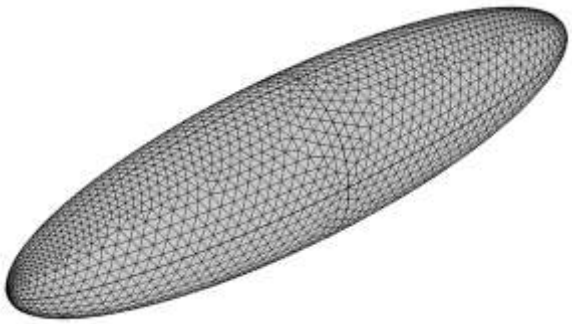

Figure 4.1 Three-dimensional meshed model geometry of rough rice in Comsol Multiphysics® simulation program.

4.3.6 Thermo-physical Parameters of Drying Air and Rough Rice

The length, width, and thickness of the rough rice was determined using a digital caliper with accuracy of 0.01 mm. Pereira et al. (2015) reported the values of thermo-physical parameters of rough rice as following: density ρ = 658.75 kg/m^3, thermal conductivity k = 0.11042 W/m.K, specific heat c_p = 1916.4 J/kg.K. Air parameters used in the simulation of rough rice drying are presented in Table 4.2. Air flow rate of IGAsorp was 250 mL/min. Dividing the air flow rate (4.16 × 10^{-6} m^3/s) with the surface area of rice kernel (A = 3.76 × 10^{-5} m^2) gives the air velocity v = 0.11 m/s. The values of convective mass transfer coefficient and convective heat transfer coefficient were calculated to be 3.9 × 10^{-7} (m/s) and 34.8 W/m^{2}K, respectively.

Table 4.2 Thermo-physical properties of air used in the simulations of the rough rice drying.

Air Parameters	**Values**
Density (kg/m^3)	1.22
Viscosity (kg/ms)	1.85e^{-5}
Specific heat (J/kg.K)	1012
Thermal conductivity (W/mK)	0.02
Vapor diffusivity (m^2/s)	2e-5
Flow rate (m^3/s)	4.16e^{-6}
Temperature (ºC)	5, 15, 30
Relative humidity (%)	40, 50

4.3.7 Thin Layer Mathematical Models

Moisture sorption isotherms of hybrid long-grain rice cultivar XL-745 at chilled environment were modeled as $M_e = f(RH, T)$. Results of rough rice MC during adsorption and desorption versus temperature and RH were analyzed using nonlinear regression in JMP Pro 14 (SAS Institute Inc., Cary, NC) to estimate the empirical constants (*A*, *B*, and *C*) of the mathematical equations listed in Table 4.3.

Table 4.3 Equilibrium models used for describing grain sorption data.

Equation	Equilibrium Moisture Content Model
Modified Chung-Pfost (Chung & Pfost, 1967)	$M_e = \frac{-1}{C}\ln\left[\left(\frac{-(T+B)}{A}\right)\ln RH\right]$
Modified Henderson (Henderson, 1952)	$M_e = \left[-\frac{ln(1-RH)}{A(T+B)}\right]^{\frac{1}{C}}$
Modified Halsey (Halsey, 1948)	$M_e = \left[-\frac{exp(A+B\ .\ T)}{\ln RH}\right]^{\frac{1}{C}}$
Modified Oswin (Oswin, 1946)	$M_e = (A+B\ .\ T)\left[\frac{RH}{1-RH}\right]^{\frac{1}{C}}$
Modified GAB (Jayas & Mazza, 1993)	$M_e = \frac{A\ .\ B\ .\left(\frac{C}{T}\right)\ .\ RH}{(1-B\ .\ RH)\left[1-B\ .\ RH+\left(\frac{C}{T}\right).B\ .RH\right]}$

4.3.8 Statistical Analysis

Parameters of each model were determined by non-linear regression. The quality of fitting of experimental data to the selected mathematical models was tested with a root means square error (RMSE). The RMSE between the predicted and measured EMC results were calculated and compared. The lower the value of RMSE, the more precise the model (Chapra and Canale, 2010). In addition, Excel software (Microsoft Office 2019, Microsoft Corp., Redmond, Wash.) was used to calculate the Percent bias (PBIAS). The PBIAS measures the average tendency of the predicted

data to be larger or smaller than their observed counterparts (Gupta et al., 1999). The optimal value of PBIAS is 0.0, with a lower magnitude indicating a more accurate model prediction. Positive values indicate a model bias toward underestimation, whereas negative values indicate a bias toward overestimation. RMSE and PBIAS were calculated as follows:

$$RMSE = \sqrt{\frac{\sum_{i=1}^{N}\left(M_e^i - M_p^i\right)^2}{N}} \quad \text{Eq 4.25}$$

$$PBIAS = \frac{\sum_{i=1}^{N}\left(M_e^i - M_p^i\right) * 100}{\sum_{i=1}^{N}\left(M_e^i\right)} \quad \text{Eq 4.26}$$

Where M_e is the experimental EMC, M_p is the predicted EMC, N is the number of experimental data point, i is the i^{th} data point out of the N total points.

4.4 Results and Discussion

4.4.1 Moisture Sorption Isotherms

The sorption isotherms of long-grain hybrid rice cultivar XL-745 at chilled environment and RHs ranging from 10% to 70% obtained by IGAsorp analyzer, is shown in Figure 4.2. This figure demonstrates that at a constant temperature, there is a positive correlation between EMC and the %RH of the rough rice; where an increase in %RH was accompanied by an increase in the EMC. These results indicate that, the sorption relation of rice can be reasonably elucidated by a sigmoidal shape which has been observed by several authors for starchy foods including rice (Togrul and Arslan, 2006; Blahovec and Yanniotis, 2009; Atungulu et al., 2016).

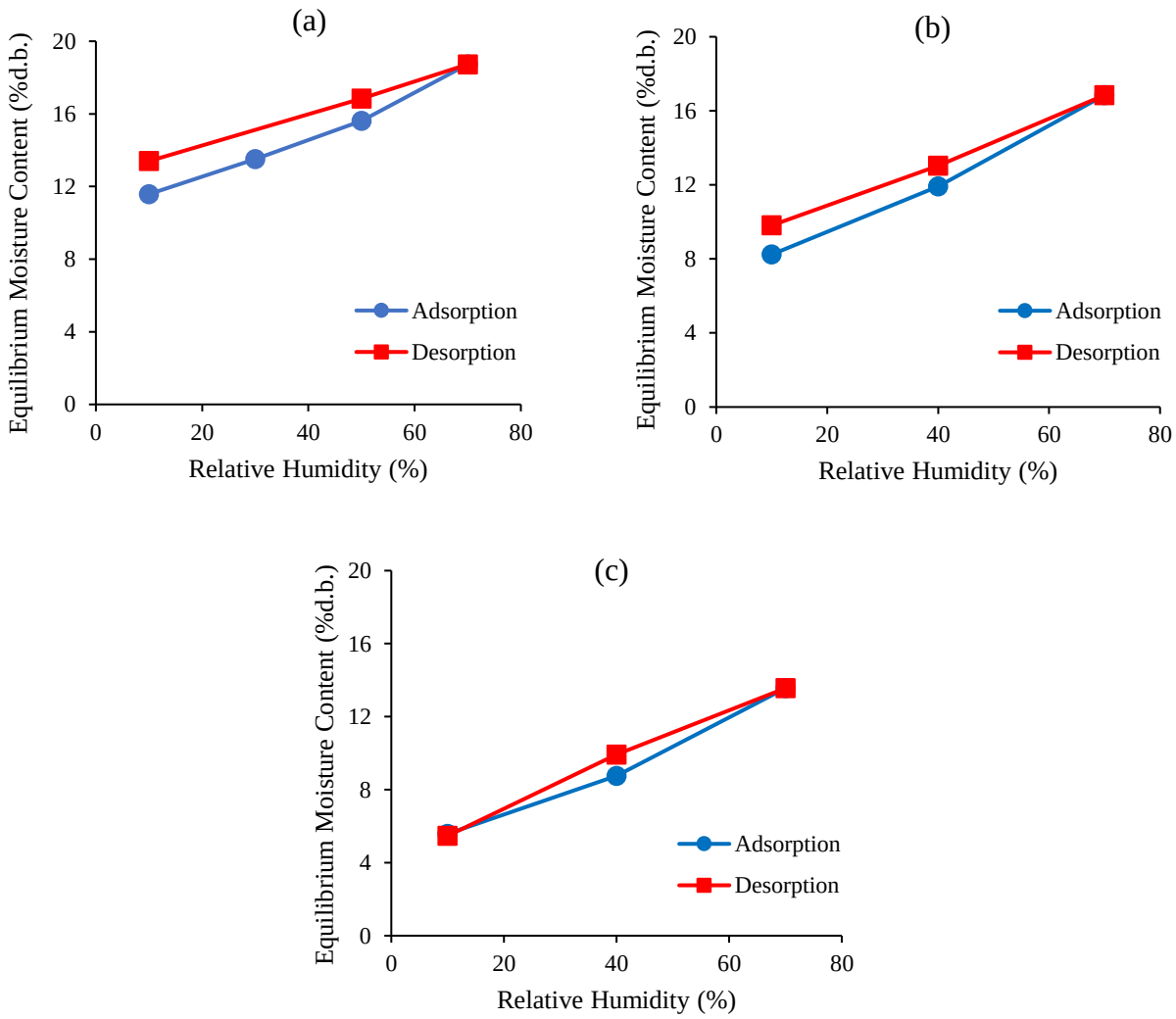

Figure 4.2 Sorption isotherms of long-grain hybrid rice cultivar XL-745 at (a) 5ºC, (b) 15ºC, and (c) 30ºC.

Table 4.4 Equilibrium moisture content experimental values for adsorption, desorption and hysteresis of long-grain hybrid rice cultivar XL-745.

Temperature (ºC)	**RH (%)**	**EMC of adsorption (% d.b.)**	**EMC of desorption (% d.b.)**	**Hysteresis (% d.b.)**
5	**10**	11.6	13.4	1.8
5	**50**	15.6	16.8	1.2
15	**10**	8.2	9.8	1.6
15	**40**	11.9	13.0	1.1
30	**10**	5.5	5.6	0.1
30	**40**	8.7	9.9	1.2

Table 4.4 shows temperature and RH values used in the experiment, along with the EMC values for long-grain hybrid rice cultivar XL-745 experimental data obtained for desorption and adsorption, and hysteresis magnitudes. Comparing EMC values for desorption and adsorption, for all air conditions used leads to the conclusion that values acquired for desorption are always higher than those obtained for adsorption. One of the accepted theories regarding the hysteresis phenomenon suggests that, during adsorption, the rice kernel porous region formed by capillaries begins to swell up, due to the increase in RH. Once the partial pressure of the air's water vapor becomes higher than the capillary's vapor pressure, water moves towards the pore interior. Meanwhile during desorption, the pore is saturated at the beginning of the process. When the partial pressure of the surrounding air's water vapor is lower than the vapor pressure inside the capillary, water diffuse from boundary to surface of the rice kernel (Zeymer et al., 2019). According to Table 4.4 hysteresis magnitudes decrease as temperature increases which is also reported by several authors (Benado and Rizvi, 1985; McLaughlin and Magee, 1998). However, hysteresis value at 30ºC was 0.6% d.b. higher than hysteresis at 15ºC, at 40% RH, probably due to the elasticity increase of the capillary walls. Similar result was encountered by Zeymer et al. (2019) studying sorption isotherms of paddy rice grains at temperatures 10, 20, 30, 40 and 50ºC. Zeymer et al. (2019) reported that hysteresis values at 30ºC were higher than hysteresis at 20ºC, at the water activity interval between 0.3 and 0.4. There is no concrete explanation for the hysteresis loop, it is commonly believed that there should be some irreversible thermodynamic reactions responsible for the changes of sorption characteristic of food (Rahman and Al-Belushi, 2006; Mousa et al., 2014). Mohsenin (1986) reported that the dehydration of food material caused an increase of hydrophobic particles on its surface which makes the reduction of water holding capacity in a further cycle of adsorption.

According to the EMC values of rice decreased as the temperature was increased at constant RH. The impact of temperature on the sorption capacity of rice was less in the adsorption data compared to the desorption data. The increase in EMC at the lower temperature can be explained by the following reasons: 1) kinetic energy the water molecules are holding is insufficient to free them from their corresponding sorption sites (Quirijns et al., 2005); 2) water molecules have hydrogen bounds along with hydrophilic groups of the biopolymer such as starch and proteins (Slade and Levine, 1991).

Due to the hygroscopic nature of rice kernel, it responds to moisture changes by expanding or shrinking. Kunze and Calderwood (1985) reported that the rapid changes in moisture content might increase the risk of fissuring in rice kernels. Therefore, the rate of adsorption/desorption of rice kernels in different RHs and temperatures is critical for rice processors to minimize the risk of fissuring. In this study, the rate of the equilibration was about 0.001 mg/min to obtain the high accuracy equilibration curve. Bingol et al. (2012) suggested that at a certain RH level equilibration rate for DVS method is faster than static method and the duration to obtain a full isotherm depends on the number of RH steps during which the product needs to reach the moisture equilibrium.

Figure 4.3 illustrates the effects of different isotherms at studied RHs and temperatures on the moisture ratio of rough rice. All the drying curves showed that the whole drying of rough rice occurs in the falling rate period. The results showed that the rice kernel absorb and desorb moisture faster when the RH is high. It is clearly seen from Figure 4.3 that rice kernel at 5ºC with 10% RH, absorbs and desorbs moisture slowly.

Figure 4.4a and Figure 4.4b show the comparison of adsorption and desorption rates of long-grain hybrid rice cultivar XL-745 at temperatures studied (5ºC, 15ºC, 30ºC) and RH ranging from 10% to 70%. It is clearly seen from Figure 4.4 that the moisture changes during the first 100 hours of

adsorption/desorption of rough rice at 30ºC was higher than those at 5ºC. Kannan et al. (1995) reported that the effect of drying air temperature on drying rate is related to the increase of intra-particle moisture transport as the particle temperature increases. With the increase of air temperature, the duration needed to achieve desired moisture content decreased (Khanali et al., 2016). The higher rate of drying during early stages of drying is attributed to the higher rate of moisture diffusion to the material surface, due to the high moisture content during initial stages of drying. Moreover, RH could change the rate of adsorption and desorption. The rate of rice kernels absorption/desorption was higher when the RH was high. Among the air conditions studied, drying air at 30ºC and 70% RH had high (>1.4%) rate of adsorption. However, drying air at 5ºC and 30% RH had low (<1.1%) rate of adsorption. The sudden increase in ambient RH, especially over 40% RH, caused significant moisture gradients. However, changes in ambient conditions below 40% RH might not cause fissuring since rice kernel absorb and desorb moisture slowly, therefore the moisture gradients could be assumed to be too low to cause fissuring (Bingol et al., 2012).

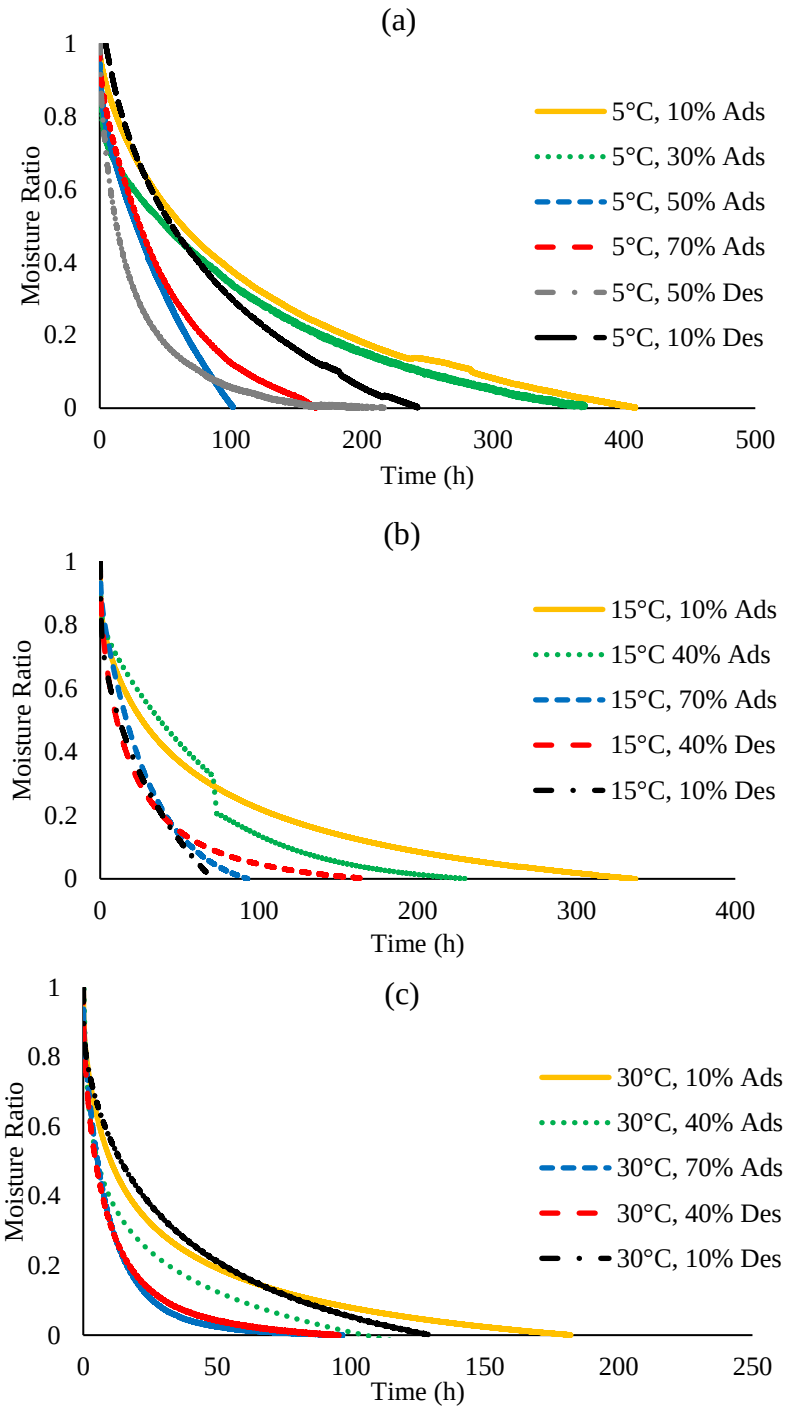

Figure 4.3 Comparison of moisture ratios of long-grain hybrid rice cultivar XL-745 at different drying air conditions: (a) 5ºC, (b) 15ºC, and (c) 30ºC. Ads and Des indicates adsorption and desorption, respectively.

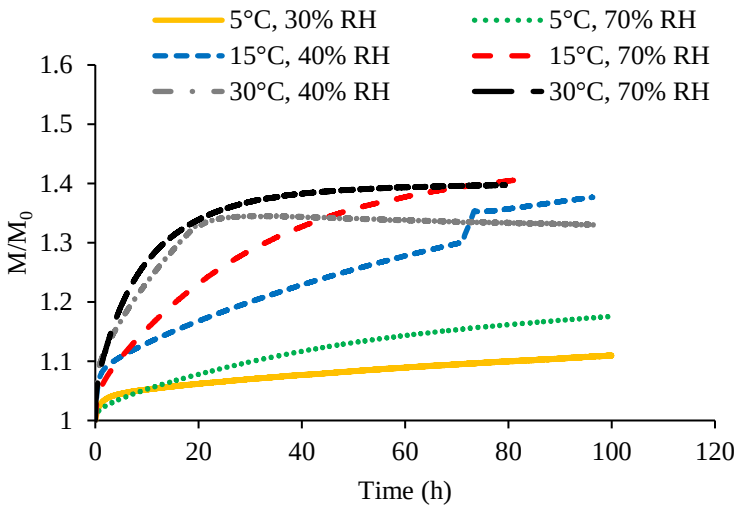

(a)

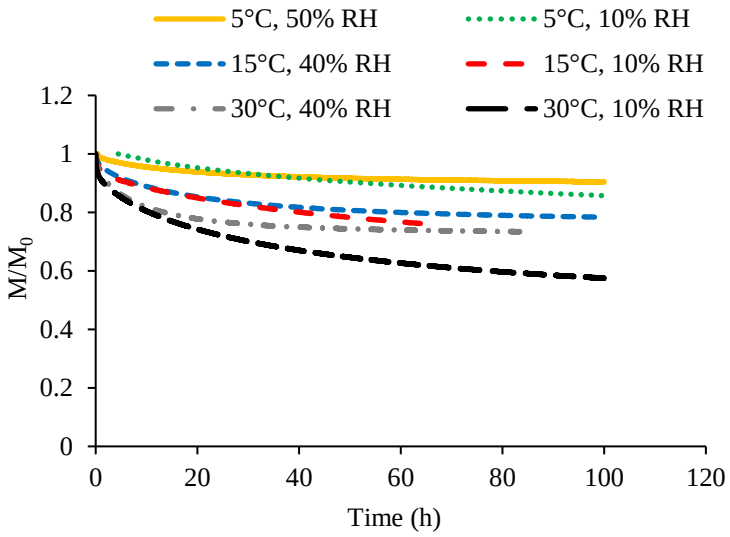

(b)

Figure 4.4 Comparison of rates of (a) adsorption and (b) desorption of moisture for long-grain hybrid rice cultivar XL-745 subjected to studied temperatures (5, 15, and 30ºC). M: moisture content at time t (g/100 g dry matter); M_0: initial moisture content at respective relative humidity (g/100 g dry matter).

4.4.2 Effective Moisture Diffusivity and Energy of Activation

The D_{eff} values for rough rice drying were calculated based on Eq 4.5 and are presented in Table 4.5. Srinivasakannan et al. (1994) reported that the effective moisture diffusivity for food material is mostly in order of $10^{-8} – 10^{-12}$ m^2/s. The diffusion coefficient is affected by various factors such

as 1) variety, 2) geometry and 3) ambient air conditions (Cihan et al., 2008). Khanali et al. (2016) reported the effective moisture diffusivity values of fluidized bed drying of rough rice in the range of 4.8×10^{-11} to 1.4×10^{-10} m^2/s. Steffe and Singh (1982) reported the values of effective moisture diffusivity for convective drying of rough rice in the range of 4.7×10^{-12} to 6×10^{-11} m^2/s. Hacihafizoglu et al. (2008) reported that the theoretical predictions of effective moisture diffusivity based on the prolate spheroid geometry for rough rice drying are in better agreement with the experimental results as compared to those based on the spherical and finite cylindrical geometry. Lu and Sibenmorgen (1992) reported that the effective moisture diffusivity and activation energy of two cultivars of long grain rice were different even at same drying air conditions.

Increasing the drying temperature from 5ºC to 30ºC increased the moisture diffusivity from 8.2×10^{-13} to 6.4×10^{-12} m^2/s (Table 4.5). Several studies reported that the increase or decrease in effective moisture diffusivity is related to the magnitude of drying rates (Khanali et al., 2016; Cihan et al., 2008). The effective moisture diffusivity increased with increased drying temperature due to more energy being provided at higher drying temperatures, which increased the activity of water molecules and increased the drying rate. As temperature increased, the bound moisture that is distributed inside the grain with relatively strong bonding began to evaporate in the drying process (Sadaka and Atungulu, 2018).

A linear relationship between $ln\ (D_{eff})$ versus $1/T$ is presented in Figure 4.5 due to the Arrhenius type dependence. The value of the activation energy was determined by Eq 4.7 and was 25.1 kJ/mol for rough rice under isothermal drying conditions. Zogzas et al. (1996) reported that the activation energy for drying of agricultural and food materials is mostly in the domain of 12.7-110 kJ/mol. Iguaz et al. (2003) reported that the values of activation energy for thin layer drying of different varieties of rough rice are in the range of 18.5-55.4 kJ/mol. Studies have shown that the

higher activation energy is required to dry rice at lower air velocity, which means that it takes longer to dry rice at low air velocities (Iguaz et al., 2003; Khanali et al., 2016). In this study, the chilled environment (5-15ºC) and the small flow rate of drying air (250 mL/min or 0.11 m/s) could be attributed to the small value obtained for the activation energy.

Table 4.5 Effects of studied temperatures (5, 15, and 30ºC) and relative humidities (10, 30, 40, 50, and 70%) on the drying rate constant (k), moisture diffusivity (D_{eff}) and activation energy (E_a). Ads and Des indicates adsorption and desorption, respectively.

Temperature (ºC)	**RH (%)**	**Isotherm**	***k* (h^{-1})**	***D_{eff}* (m^2/s)**	***E_a* (kJ/mol)**
5	10	Ads	0.0086	9.0×10^{-13}	25.1
	30	Ads	0.0079	8.2×10^{-13}	
	50	Ads	0.0247	2.6×10^{-12}	
	70	Ads	0.0213	2.2×10^{-12}	
	50	Des	0.0248	2.6×10^{-12}	
	10	Des	0.0132	1.4×10^{-12}	
15	10	Ads	0.011	1.1×10^{-12}	
	40	Ads	0.019	2.0×10^{-12}	
	70	Ads	0.0432	4.5×10^{-12}	
	40	Des	0.0272	2.8×10^{-12}	
	10	Des	0.0429	4.5×10^{-12}	
30	10	Ads	0.022	2.3×10^{-12}	
	70	Ads	0.0615	6.4×10^{-12}	
	40	Des	0.051	5.3×10^{-12}	
	10	Des	0.0277	2.9×10^{-12}	

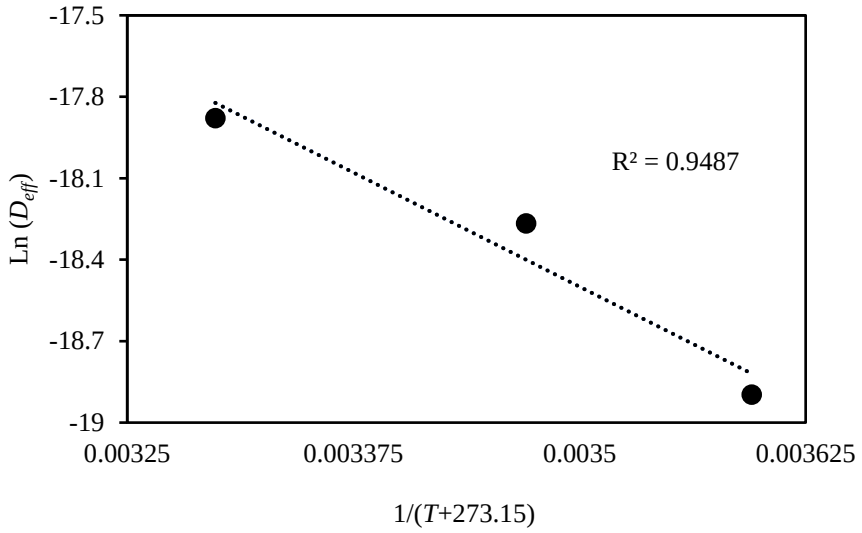

Figure 4.5 Arrhenius type relationship between D_{eff} and reverse of absolute drying temperature.

4.4.3 Modeling Sorption Isotherm

The parameters of the sorption models for the adsorption and desorption of long-grain hybrid rice cultivar XL-745 along with the RMSE are presented in Table 4.6. Based on minimizing RMSE, for temperatures ranging from 5ºC to 30ºC and RHs from 10% to 70%, the modified Chung-Pfost equation was found to be the most accurate model for describing EMC for both adsorption and desorption data of rice samples. However, the modified Oswin and modified Halsey equations gave nearly identical RMSE values for adsorption (<0.95) and desorption data (<1.2). Moreover, modified Oswin and modified Halsey equations were superior to the other two EMC models (modified Henderson and modified GAB) when describing EMC data. Several studies reported the modified Chung-Pfost equation to be the most appropriate in describing EMC of rough rice at temperatures ranging from 10ºC to 60ºC (Sun, 1999; Basunia and Abe, 2001; Iguaz and Versada, 2007; Ondier et al., 2011). Ondier et al. (2011) reported RMSE values for describing EMC data followed by the modified Chung-Pfost, modified GAB, modified Oswin, modified Halsey, and modified Henderson equations of hybrid long-grain rice (XL-730) as following 0.736, 0.724, 0.862, 0.995, and 0.948, respectively.

Sorption isotherms of rough rice determined by the EMC equations (Table 4.3) for temperatures of 5, 15, and 30ºC are shown in Figure 4.6a, 4.6b, respectively. The experimental EMC values at 5ºC were generally more than those of predicted equations especially at RH less than 40%. However, no significant differences were observed between the measured rough rice EMCs and EMCs predicted from the equations at 30ºC and all RHs. Ondier et al. (2011) reported the EMC values of hybrid long-grain rice (XL-730) at drying air temperature of 30ºC and RHs of 10%, 50%, and 70% as following 5.04% d.b, 11.6% d.b, and 14.8 % d.b., respectively.

Based on RMSEs of sorption isotherms of rough rice, modified Chung-Pfost equation was recommended to describe the EMC isotherms of rice in the range of experiments (5-30ºC and 10-70% RH). Table 4.7 shows the PBIAS values between measured EMC values and predicted EMC values from modified Chung-Pfost equation for temperatures at 5, 15, and 30ºC. The PBIAS results showed that predicted EMC values overestimated the actual EMC values by 14.8% and 8.7% for samples at 5ºC and 15ºC, respectively. However, the PBIAS value at temperature 30ºC is negative which means that the model underestimates the results by 7.9%. Since the values closer to zero are preferred for PBIAS, the modified Chung-Pfost equation accurately predicted rough rice EMC values at temperatures higher than 15ºC.

Table 4.6 Estimated coefficients of the modified Chung-Pfost, modified Henderson, modified Halsey, modified Guggenheim Anderson DeBoer (GAB), and modified Oswin equations, and the statistical parameters used to evaluate the models. RMSE has unit % (d.b.), which is the same as the unit of the response variable (equilibrium moisture content) of the regression model.

		Estimated Model Constants			**Statistical Coefficient**
Model	**Isotherm**	A	B	C	RMSE
Modified Chung-Pfost	Adsorption	297.4197	4.8974	0.2340	0.557
	Desorption	383.3781	0.4815	0.2630	0.912
Modified Henderson	Adsorption	$3.1561e^{-6}$	3.2386	3.6403	1.213
	Desorption	$8.1625e^{-8}$	-2.977	5.3102	1.682
Modified Halsey	Adsorption	8.0843	-0.052	2.9750	0.855
	Desorption	10.9296	-0.091	3.7926	1.196
Modified GAB	Adsorption	14.6168	0.2844	430.30	1.318
	Desorption	17.4294	0.0005	249273.28	1.307
Modified Oswin	Adsorption	17.1191	-0.225	4.6861	0.947
	Desorption	18.7899	-0.317	6.8906	1.176

Table 4.7 Comparison of percent biases (PBIASs) of experimental and predicted equilibrium moisture content (% dry basis) values for rough rice at 5°C to 30°C and 10% to 70% RH.

		Equilibrium Moisture Content (% dry basis)		
Temperature (°C)	**Relative Humidity (%)**	**Present study**	**Modified Chung-Pfost**	**PBIAS (%)**
5	**10**	12.5	8.9	
	30	13.5	11.7	14.8
	50	16.2	14.2	
	70	18.7	17.1	
15	**10**	9.0	7.6	
	40	12.5	11.6	8.7
	70	16.8	15.8	
30	**10**	5.5	6.1	
	40	9.3	10.2	-7.9
	70	13.7	14.3	

* Each value is an average of adsorption and desorption for each condition.

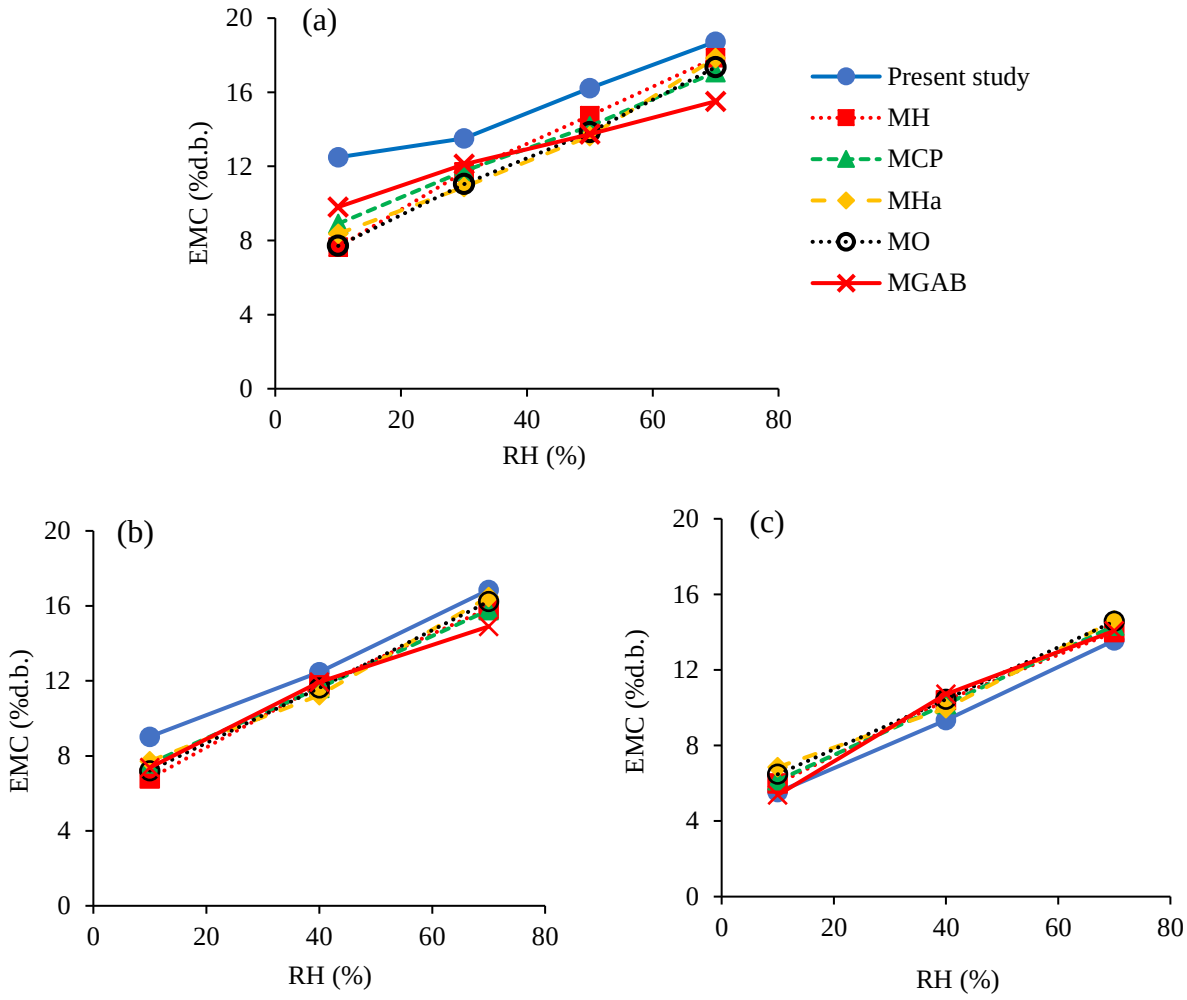

Figure 4.6 Equilibrium isotherms (expressed on a dry basis) from the present study compared to data predicted by modified Henderson (MH), modified Chung-Pfost (MCP), modified Halsey (MHa), modified Oswin (MO), and modified Guggenheim Anderson DeBoer (MGAB) for: (a) 5ºC, (b) 15ºC, and (c) 30ºC. EMC indicates equilibrium moisture content; RH indicates relative humidity; d.b. indicates dry basis.

4.4.4 Moisture and Temperature Distribution

Due to existing uncertainty on mechanism of moisture movement in the rice kernel, some researchers have assumed Dirichlet boundary condition (Meeso et al., 2007; Prakash and Pan, 2011) while others have considered Newmann boundary condition (Yang et al., 2002) for the moisture transport modeling of rice kernel. Therefore, the model was tested by comparing the

predicted average MC values at drying air temperature of 5°C, 50% RH in different boundary conditions (Figure 4.7). The results showed a high similarity between the simulated average MC at Dirichlet and Newmann boundary conditions. Due to the identical values for average MC for both boundary conditions, it can be suggest that the evaporation only occur at surface of kernel (Prakash and Pan, 2011). For the sake of ease in further simulation, the Dirichlet bounday condition was used as a selected bondary condition for moisture transport of rice kernel. In this study both heat and mass transfer were considered. However, it was observed that the surface and center temperatures only differed at first 5 hours of drying and rough rice kernel can be considred isothermal during drying process. Many other researchers also assumed grains to be isothermal during drying process and neglected heat transfer with the rice kernel (Pabis and Henderson, 1962; Prakash and Pan, 2012).

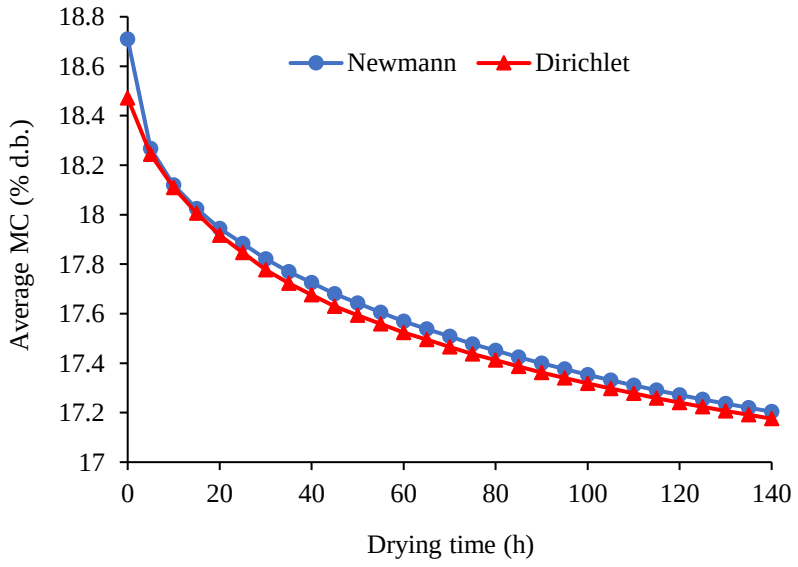

Figure 4.7 Average moisture content of rough rice during drying at 5°C, 50% relative humidity or two boundary conditions.

Simulations were run with a model assuming ellipsoid-shaped rice to determine moisture distribution within the rice kernel during drying. In these simulations, drying temperatures at chilled condition of 5°C, 50% RH and 15°C, 40% RH with initial MCs of 18.7% and 16.8% (on d.b.) respectively, were used to mimic those practiced by grain cooling systems. Moisture distribution within the rough rice kernel for drying temperature of 5°C, 50% RH and 15°C, 40% RH are shown in Figure 4.9 and Figure 4.9, respectively. It can be seen that the moisture was transferred from the kernel center to its surface, causing an inhomogeneous moisture distribution inside the kernel. Pereira et al. (2015) and Zhao et al. (2019) reported that the flux of moisture during the drying process of rough rice occurs from the center of the rice to the surface in a non-homogeneous flow. Moreover, it is observed that the moisture content of the rice kernel is reduced more quickly at the tail of rice kernel which makes it susceptible to fissuring.

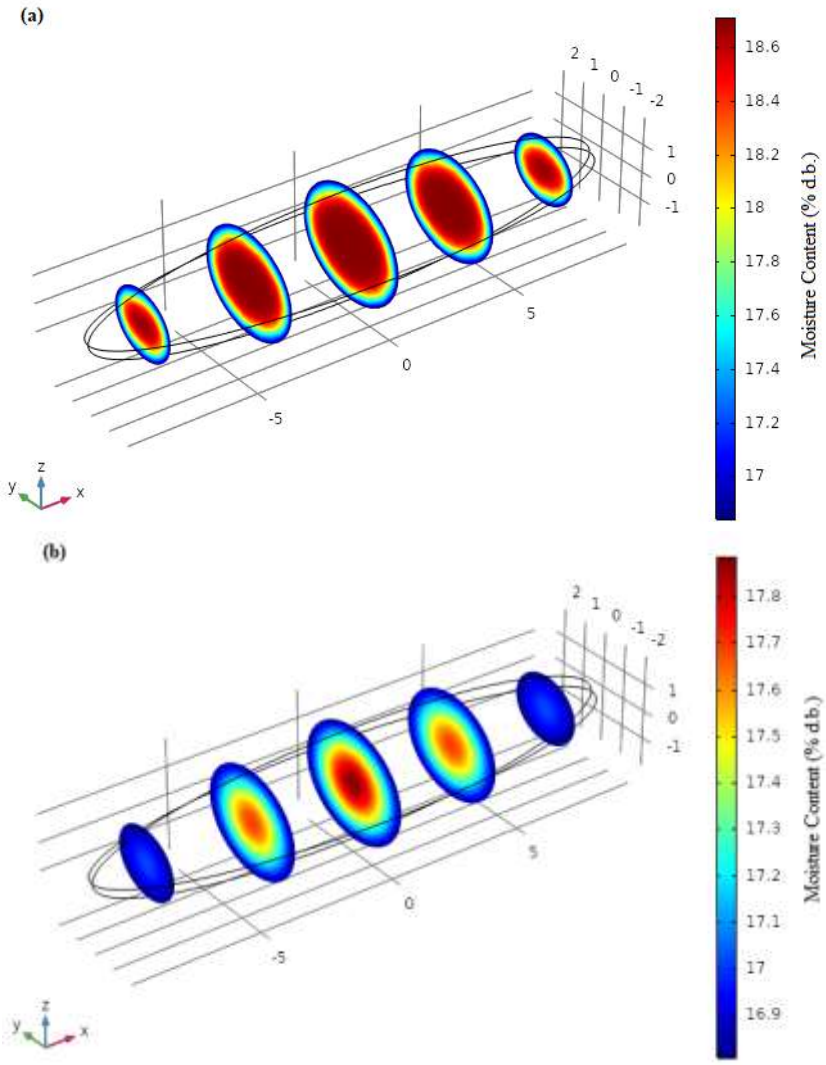

Figure 4.8 The moisture distribution inside the rice kernel in transverse planes at drying temperature of 5°C, 50% relative humidity and drying times (a) 10 h and (b) 140 h.

Moreover, the simulation was run to determine moisture gradient (MG) within the rice kernel during drying at 5°C, 50% RH and 15°C, 40% RH. As seen in Figure 4.10, only one-eighth of the actual rough rice volume was considered due to the existence of symmetry about the three axes in the rice kernel. The results showed that the maximum MG was located near the kernel surface. During drying rice kernel, the moisture diffusion boundary gradually moved from the kernel surface to the center and the mass transfer resistance got bigger (Zhao et al., 2019). In this study, the MG decreased from 40 to 10 (% d.b./mm) during first 10 hours of drying air at 5°C, 50% RH.

This reduction of MG reached to constant and slower pace after 70 h of drying due to the higher moisture transfer resistance. The maximum MG of drying air at 15°C, 40% RH was 30 % d.b./mm higher than those at drying air 5°C, 50% RH; this deviation is due to the higher drying rate at 15°C, 50% RH.

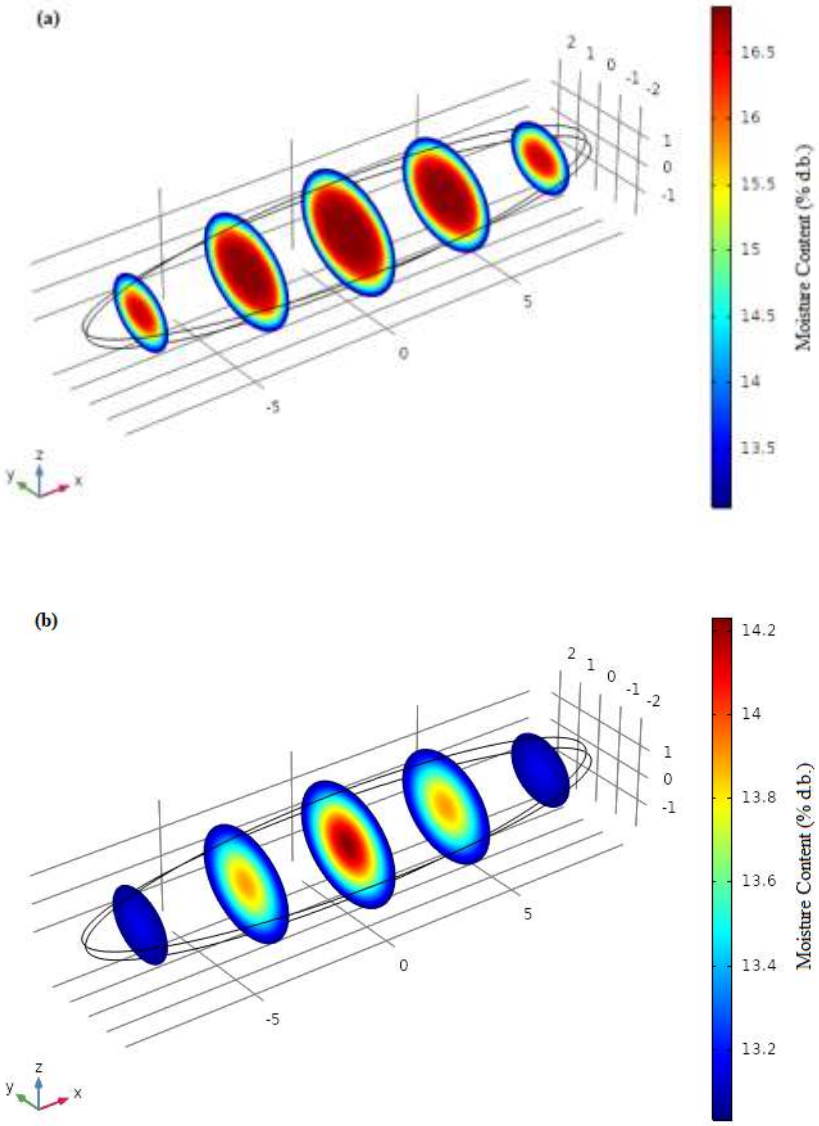

Figure 4.9 The moisture distribution inside the rice kernel in transverse planes at drying temperature of 15°C, 40% relative humidity and drying times (a) 10 h and (b) 155 h.

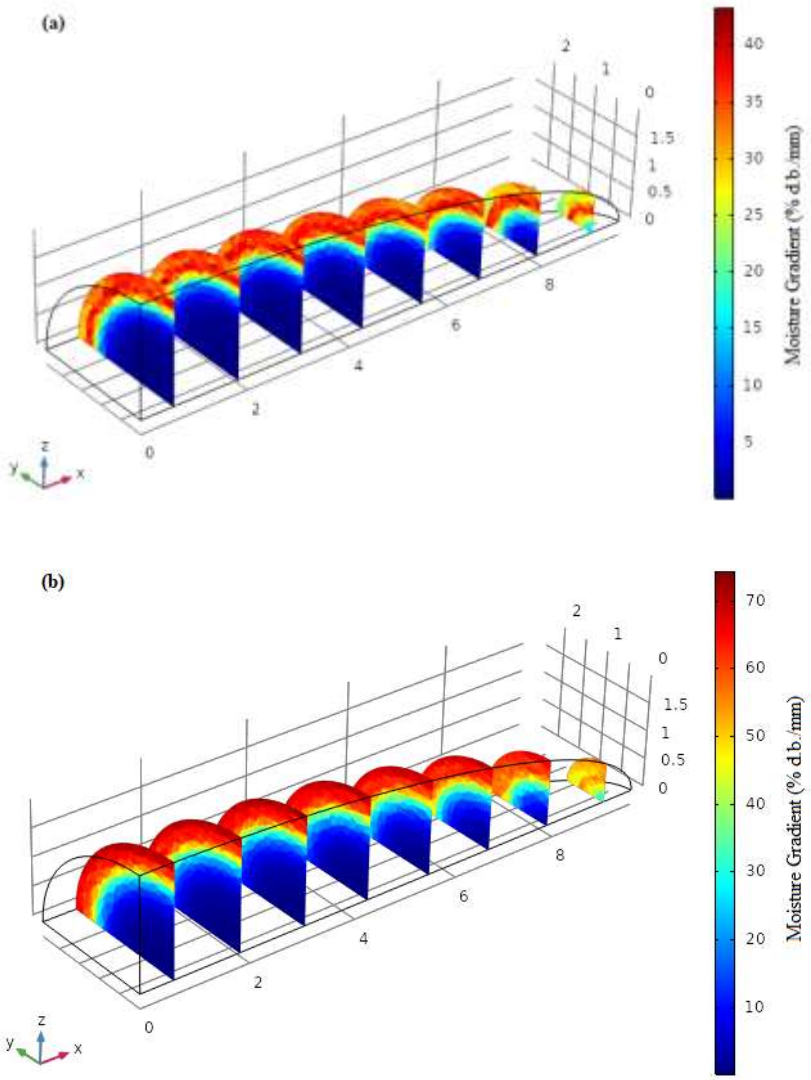

Figure 4.10 Moisture gradient in the ellipsoid shaped rough rice model (1/8 volume) after 10 h of air drying at (a) 5ºC, 50% relative humidity and (b) 15°C, 40% relative humidity.

Three specific points located in rough rice kernel (tail, core, surface) were selected as representative of the sites having moisture transfer in the model. The position of core, surface, and tail in the Cartesian system of x, y, z were (1, 0.3, 0.3 mm), (0.6, 1, 1 mm), and (-8.7, -0.1, -0.1 mm), respectively. The predicted MCs of the three points in the model during drying simulations at 5°C, 50% RH are shown in Figure 4.11. The results of the simulation illustrate that the moisture concentration in the rough rice is reduced more quickly at the tail of the rice, this being the area

most likely to fissures due to high moisture gradients in that location. However, the moisture concentration in the core of rice kernel reduced slowly.

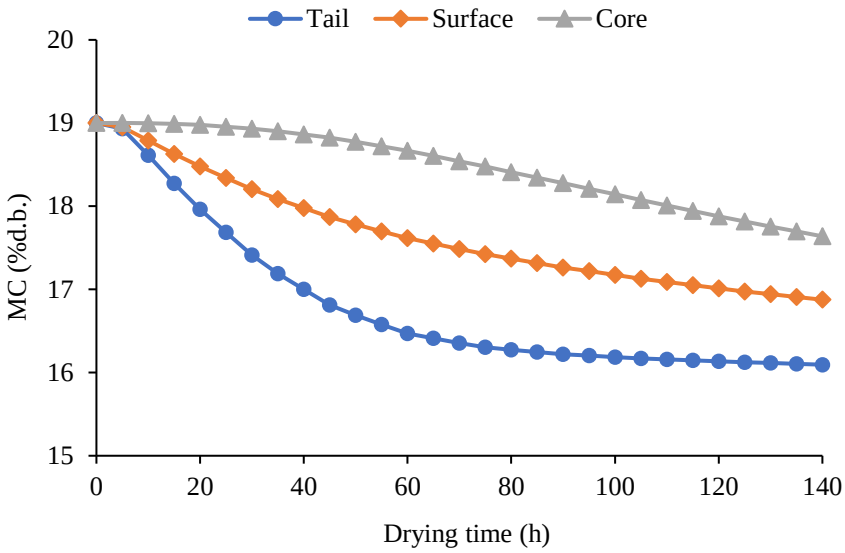

Figure 4.11 Moisture concentration at three specific points (tail, surface, core) located inside the rough rice kernel during drying at temperature of 5°C, 50% relative humidity.

Figure 4.12a and 4.12b illustrate the comparison of the experimental and simulated values of average MC of the rough rice for temperatures 5°C, 50% RH and 30°C, 40% RH, respectively. It is observed that the experimental MC values for both drying temperatures are less than simulated values. The RMSE between the experimental and simulated data for average MC at 5°C, 50% RH and 30°C, 40% RH were 0.172 and 0.518, respectively. The small error values indicate the validity of the simulation results. Meanwhile, the small difference in the values of the MC is related to shape of the grain and diffusion coefficient consideration.

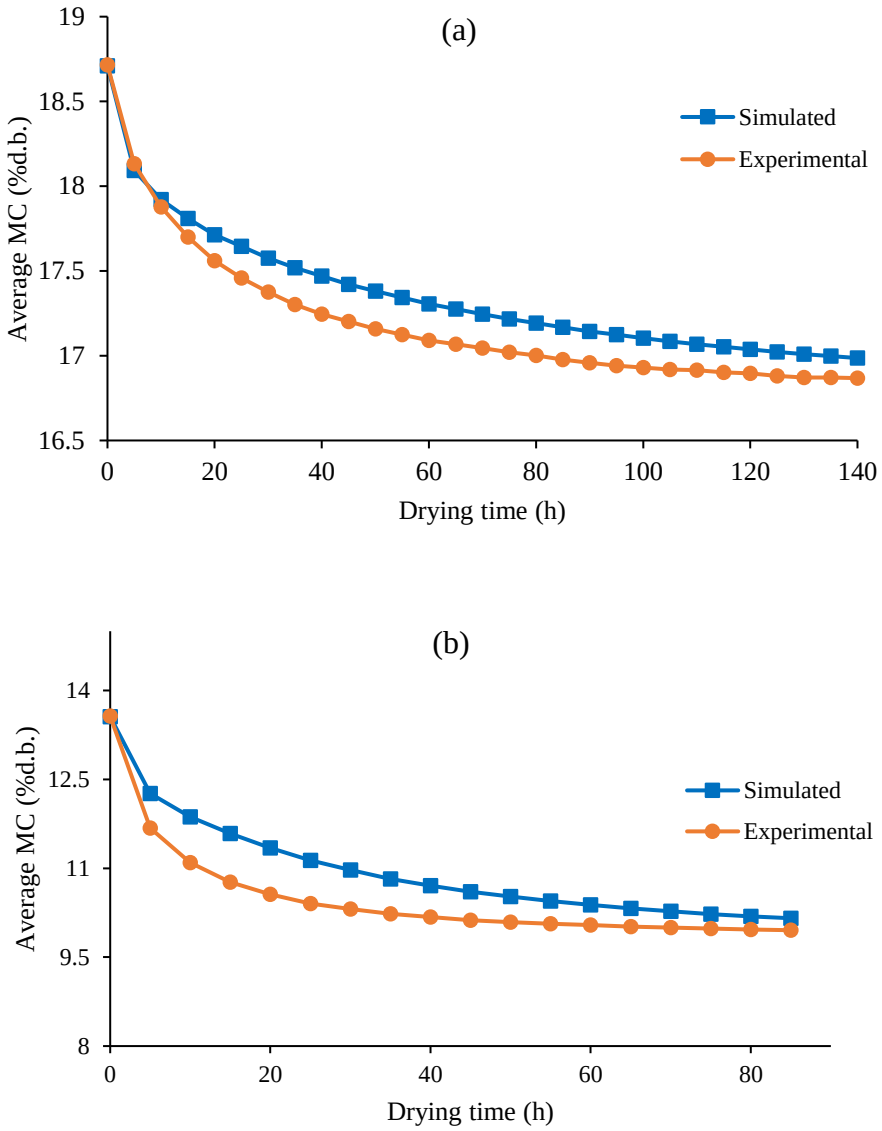

Figure 4.12 Experimental and simulated average moisture content of the rough rice for drying temperature of (a) 5°C, 50% relative humidity and (b) 30°C, 40% relative humidity.

4.5 Conclusion

In this study, adsorption and desorption isotherms of rough rice in the range of temperatures and relative humidities (RHs) commonly used in chilling aeration were determined by dynamic vapor sorption (DVS) method. At fixed RH, the equilibrium moisture content (EMC) decreased with the increase in temperature. Hysteresis was evident, and the magnitude of the hysteresis loop increased at 5ºC. The rates of adsorption/desorption of rough rice at 5ºC were less than those at 15ºC and

30ºC. Parameters of *A*, *B*, and *C* of the empirical equations were estimated. Among the five models (modified Chung-Pfost, modified Henderson, modified Oswin, modified Halsey, and modified GAB) which were evaluated for their ability to describe the experimental sorption data, the modified Chung-Pfost equation was the superior one in terms of prediction accuracy of the rice EMCs (RMSE<0.9). However, the modified Henderson was the inferior equation (RMSE>1.6). The PBIAS values of modified Chung-Pfost at 5ºC was higher than at 15ºC and 30ºC. The effective moisture diffusivity evaluated based on Fick's diffusion equation was found to vary from 9.0×10^{-13} to 1.1×10^{-12} m^2/s at drying air temperatures of 5ºC and 15ºC, respectively. The activation energy and pre-exponential factor of the Arrhenius equation of rough rice at studied temperatures (5, 15, and 30ºC) were found to be 25.1 kJ/mol and 0.0003 m^2/h, respectively. Based on mathematical model of diffusion solved by Comsol Multiphysics®, the maximum moisture gradient of rough rice during first 10 hours of drying at 5ºC, 50% RH was 40 %d.b./mm and it reduced to with the drying time. The experimental values of average MC at both drying air of 5ºC and 30ºC were compared with those simulated by the model and found to be in good agreement with each other. The knowledge of the drying kinetics and EMCs of rough rice at chilled environment could allow rice processors to determine the optimum processing conditions during chilling aeration and to improve automated monitoring of rice moisture, temperature and quality conditions.

Acknowledgement

The authors acknowledge the University of Arkansas Division of Agriculture, and the Rice and Grain Processing program for collaboration and providing facilities. The authors also acknowledge FrigorTec America Ins., especially through Jahannes Karcher for support and cooperation during the research. The authors also wish to acknowledge Mr. Mike Sullivan, Mr. Joe Mencer and Mr. Gregory O'Gary who provided rice sample and their facilities to conduct this research. This study

was based upon work that is supported, in part, by the United States Department of Agriculture National Institute of Food and Agriculture Hatch Act Funding.

4.6 References

Aguerre, R., Suarez, C., Viollaz, P. E. (1982). Drying kinetic of rough rice grain. Journal of Food Technology, 17(6): 679–686.

ASABE. (2014). ANSI/ASAE S448.2: Thin-layer drying of agricultural crops. St. Joseph, MI: ASABE.

Atungulu, G. G., Zhong, H., Osborn, G. S., Mauromoustakos, A., Singh, C. B. (2016). Simulation and validation of on-farm in-bin drying and storage of rough rice. Applied Engineering in Agriculture, 32 (6): 881-897.

Basunia, M. A., Abe, T. (2001). Moisture desorption isotherms of medium-grain rough rice. Journal of Stored Products Research, 37, 205-219.

Benado, A. L., Rizvi, S. S. H. (1985). Thermodynamic properties of water on rice as calculated from reversible and irreversible isotherms. Journal of Food Science, 50 (1): 101-105.

Bingol, G., Prakash, B., Pan, Z. (2012). Dynamic vapor sorption isotherms of medium grain rice varieties. LWT-Food Science and Technology, 48, 156-163.

Blahovec, J., Yanniotis, S. (2009). Modified classification of sorption isotherms. Journal of Food Engineering, 91, 72-77.

Brooker, D. B., Bakker-Arkema, F. W., Hall, C. W. (1992). Drying and storage of grains and oilseeds. AVI Book, New York.

Chapra, S. C., Canale, R. P. (2010). Numerical methods for engineers. Boston: McGraw-Hill Book Company, New York.

Chen, J. Y., Piva, M., Labuza, P. (1984). Evaluation of water binding capacity (WBC) of food fiber sources. Journal of Food Science, 49 (1): 59-63.

Choi, B. M., Lanning, S. B., Siebenmorgen, T. J. (2010). A review of hygroscopic equilibrium studies applied for rice. Transaction of the ASABE, 53(6): 1859-1872.

Chung, D. S., Pfost, H. B. (1967). Adsorption and desorption of water vapor by cereal grains and their products Part II: Development of the general isotherm equation. Transactions of the ASAE, 10 (4): 549-557.

Cihan, A., Kahveci, K., Hacihafizoglu, O., de Lima, A. G. B. (2008). A diffusion-based model for intermittent drying of rough rice. Heat & Mass Transfer, 44 (8): 905-911.

Cnossen, A. G., Siebenmorgen, T. J., Yang, W. (2002). The glass transition temperature concept in rice drying and tempering: effect on drying rate. Transaction of the ASABE, 45 (3): 759-766.

Crank, J. (1975). The mathematics of diffusion. New York: Oxford University Press.

Dadali, G., Apar, D., Ozbek, B. (2007). Estimation of effective moisture diffusivity of okra for microwave drying. Drying Technology, 25 (9): 1445-1450.

Ece, M. C., Cihan, A. (1993). A liquid diffusion for drying rough rice. Transactions of the ASAE, 36, 837-840.

Fortes, M., Okos, M. R., Barrett Jr, J. R. (1981). Heat and mass transfer analysis of intra-kernel wheat drying and rewetting. Journal of Agricultural Engineering Research, 26 (2): 109-125.

Furmaniak, S., Terzyk, A. P., Golembiewski, R., Gauden, P. A., Czepirski, L. (2009). Searching the most optimal model of water sorption on foodstuffs in the whole range of relative humidity. Food Research International, 42, 1203-1214.

Goneli, A. L. D., Correa, P. C., Martins, M. A. (2007). Moisture sorption hysteresis of rough rice. ASABE Paper No. 076194. St. Joseph, Mich.: ASABE

Gupta, H. V., Sorooshian, S., Yapo, P. O. (1999). Status of automatic calibration for hydrologic models: Comparison with multilevel expert calibration. Journal of Hydrologic Engineering, 4 (2): 135-143.

Hacihafizoglu, O., Cihan, A., Kahveci, K., O., de Lima, A. G. B. (2008). A liquid model for thin-layer drying of rough rice. European Food Research & Technology, 226 (4): 787-793.

Halsey, G. (1948). Physical adsorption on non-uniform surfaces. The Journal of Chemical Physics, 16, 931-937.

Henderson, S. M. (1952). A basic concept of equilibrium moisture. Agricultural engineering, 33, 29-32.

Igathinathane, C., Chattopadhyay, P. K. (1999). Moisture diffusion modelling of drying in parboiled paddy components. Part II: Bran and husk. Journal of Food Engineering, 41(2): 89-101.

Iguaz, A., San Martin, M. B., Mate, J. I., Fernandez, T., Virseda, P. (2003). Modelling effective moisture diffusivity of rough rice (Lido cultivar) at low temperatures. Journal of Food Engineering, 59, 253-258.

Iguaz, A., Rodriguez, M., Virseda, P. (2006). Influence of handling and processing of rough rice on fissures and head rice yields. Journal of Food Engineering, 77, 803-809.

Iguaz, A., Virseda, P. (2007). Moisture desorption isotherms of rough rice at high temperatures. Journal of Food Engineering, 79, 794-802.

Jayas, D. S., Mazza, G. (1993). Comparison of five, three-parameter equations for description of adsorption data of oats. Transaction of the ASABE, 36 (1): 119-125.

Khanali, M., Banisharif, A., Rafiee, S. (2016). Modeling of moisture diffusivity, activation energy and energy consumption in fluidized bed drying of rough rice. Heat & Mass Transfer, 52, 2541-2549.

Kunze, O. R., Calderwood, D. L. (1985). Rough rice drying. In B. O. Juliano (Ed.), Rice chemistry and technology (pp. 233-263). Minnesota: American Association of Cereal Chemists.

Lu, R., Siebenmorgen, T. J. (1992). Moisture diffusivity of long-grain rice components, Transactions of the ASAE, 35 (6): 1955-1961.

McLaughlin, C. P, Magee, T. R. A. (1998). The determination of sorption isotherm and the isosteric heats of sorption for potatoes. Journal of Food Engineering, 35 (3): 267-280.

Meeso, N., Nathakaranukule, A., Madhiyanon, T., Soponronnarit, S. (2007). Modeling of far-infrared irradiation in paddy drying process. Journal of Food Engineering, 78, 1248-1258.

Minnick, D. L., Turnaoglu, T., Rocha, M. A., Shiflett, M. B. (2018). Review article: Gas and vapor sorption measurements using electronic beam balances. Journal of Vacuum Science & Technology A Vacuum Surfaces and Films, 36 (5): 050801.

Mohsenin, N. N. (1986). Physical properties of plant and animal materials. Gordon and Breach, New York.

Mousa, W., Ghazali, F. M., Jinap, S., Ghazali, H. M., Radu, S. (2014). Sorption isotherms and isosteric heats of sorption of Malaysian paddy. Journal of food science and technology, 51 (10): 2656-2663.

Ondier, G. O., Siebenmorgen, T. J., Bautista, R. C., Mauromoustakos, A. (2011). Equilibrium moisture contents of pureline, hybrid, and parboiled rice. Transaction of the ASABE, 54 (3): 1007-1013.

Ondier, G. O., Siebenmorgen, T. J., Mauromoustakos, A. (2012). Equilibrium moisture contents of pureline, hybrid, and parboiled rice kernel fractions. Applied Engineering in Agriculture, 28 (2): 237-247.

Oswin, C. R. (1946). The kinetics of package life. III. The isotherm. Journal of the Society of Chemical Industry, 65 (12): 419-421.

Pabis, S., Henderson, S. M. (1962). Grain drying theory III. The air/grain temperature relationship. Journal of Agricultural Engineering Research, 7 (1): 21-26.

Pereira, E. M. A., da Silva, J. V., de Andrade, T. H. F., de Farias Neto, S. R., Barbosa de Lima, A. G. (2015). Simulating heat and mass transfer in drying process: Applications in grains. Diffusion Foundations, 3, 3-18.

Prakash, B., Pan, Z. Modeling moisture movement in rice. In Advance Topics in Mass Transfer; El-Amin, M., Ed.; Intech Open Access Publisher: Rijeka, Croatia, 2011; 283-304.

Prakash, B., Bingol, G., Pan, Z. (2011). Moisture diffusivity in rice components during absorption and desorption. Drying Technology, 29, 939-945.

Prakash, B., Pan, Z. (2012). Effect of geometry of rice kernels on drying modeling results. Drying Technology, 30 (8): 801-807.

Prakash, B., Mukhopadhyay, S., Siebenmorgen, T. J. (2017). Mathematical modeling of a cross-flow rice dryer. Transaction of the ASABE, 60 (3): 999-1009.

Prakash, B., Siebenmorgen, T. J. (2018). Single-parameter thin layer drying equations for long grain rice. Transaction of the ASABE, 61 (2): 733-742.

Quirijns, E. J., Van Boxtel, A. J., van Loon, W. K., Van Straten, G. (2005). Sorption isotherms, GAB parameters and isosteric heat of sorption. Journal of the Science of Food and Agriculture, 85 (11): 1805-1814.

Rahman, M. S., Al-Belushi, R. H. (2006). Dynamic Isopiestic Method (DIM): Measuring moisture sorption isotherm of freeze-dried garlic powder and other potential uses of DIM. International of Food Properties, 9, 421-437.

Rahman, M. S., Sablani, S. S. (2009). Water activity measurement methods of foods. Food properties handbook, 9-32.

Sadaka, S., Atungulu, G. G. (2018). Grain sorghum drying kinetics under isothermal conditions using thermogravimetric analyzer. Bio Resources, 13(1): 1534-1547.

Schmidt, S. J. Lee, J. W. (2012). Comparison between water vapor sorption isotherms obtained using the new dynamic dewpoint isotherm method and those obtained using the standard saturated salt slurry method. International Journal of Food Properties, 15 (2): 236-248.

Slade, L., Levine, H. (1991). A polymer science approach to structure/ property relationships in aqueous food systems: Non-equilibrium behavior of carbohydrate-water systems. In H. Levine & L. Slade (Eds.). Water Relationships in Foods. New York, NY: Plenum Press, pp. 29-101.

Srinivasakannan, C., Subbarao, S., Varma, Y. B. G. (1994) A kinetic model for drying of solids in batch fluidized beds. Industrial & Engineering Chemistry Research, 33 (2): 363-370.

Steffe, J. F., Singh, R. P. (1980). Liquid diffusivity of rough rice components. Transactions of the

ASAE, 23 (3): 767-774.

Steffe, J. F., Singh, R. P. (1982) Diffusion coefficients for predicting rice drying behavior. Journal of Agricultural Engineering Research, 27 (6): 489-493.

Sun, Da.-W. (1999). Comparison and selection of EMC/ERH isotherm equations for rice. Journal of Stored Products Research, 35, 249-264.

Togrul, H., Arslan, N. (2006). Moisture sorption behavior and thermodynamic characteristics of rice stored in a chamber under controlled humidity. Biosystems Engineering, 95 (2): 181-195.

Wellingford, L., Labuza, T. P. (1983). Evaluation of the water binding properties of food hydrocolloids by physical/chemical methods and in a low-fat meat system. Journal of Food Science, 48 (1): 1-5.

Wu, B., Yang, W., Jia, C. (2004). A three-dimensional numerical simulation of transient heat and mass transfer inside a single rice kernel during the drying process. Biosystems Engineering, 87 (2): 191–200.

Yang, W., Jia, C., Siebenmorgen, T. J., Howell, T. A., Cnossen, A. G. (2002). Intra-kernel rice moisture responses to drying and tempering treatments by finite element simulation. Transaction of the ASAE, 45 (4): 1037-1044.

Zeymer, J. S., Correa, P. C., Oliveira, G. H. H., Baptestini, F. M., Campos, R. C. (2019) Mathematical modeling and hysteresis of sorption isotherms for paddy rice grains. Engenharia Agricola, Jaboticabal, 39 (4): 524-532.

Zhao, L., Yang, J., Du, T., Wu, Z. (2019). A 3-Dimensional body fitted simulation of heat and mass transfer in rice kernel during hot air-drying process. International Journal of Food Engineering, 15 (3-4): 1-11.

Zogzas, N. P., Moroulis, Z. B., Marinos-kouris, D. (1996) Moisture diffusivity data compilation in foodstuffs. Drying Technology, 14 (10): 2225-2253.

Chapter 5: **Overall Conclusion**

Much of this research focused on engineering new methods for maintaining the quality of rice during post-harvest storage. On a major number of farms, the bottleneck is the limitations of commercial and on-farm dryer capacities during peak harvesting seasons that impedes harvesting the entire rice crop at the optimal harvest moisture content; the result is significant quality degradation and subsequent profit losses by growers. Pre-chilling the freshly harvested rice and proceeding with storage at low temperatures, and then completing the drying later using commercial dryers to attain the final/desired moisture content for storage, may help producers overcome this bottleneck in drying capacity. Moreover, the rice processing industry faces a continual challenge to prevent various forms of chemical and physical degradation in order to maintain quality at its highest level. Chilling of rice could be an attractive non-chemical treatment technology which may prevent spoilage and insect infestation, especially for on-farm, in-bin rice management. The idea behind this research was to determine how long high moisture chilled rice will keep quality. Such information will allow us to know how long the rice can stay before soaking and steaming. This will help us determine whether it is possible to eliminates one drying step in the parboiled milled rice processing; this may potentially save overall energy expenditure. Whether this approach is more economical for the mid-southern states' weather conditions or elsewhere within the rice growing region has been a research gap. Moreover, traditional on-farm, in-bin driers can be fitted with grain chillers to reduce field heat thereby helping to maintain the milled rice quality, especially minimizing the risk of discoloration which is typical in on-farm bin dried rice. The research used experimentation and massive simulation and modeling of the described operations to answer vital questions which help improve economics of rice drying and maintaining the rice quality.